AD_____

Award Number: DAMD17-02-1-0664

TITLE: Analysis of Keratin Filament Assembly/Disassembly and Structure Following Modification by Sulfur Mustard Analogs

PRINCIPAL INVESTIGATOR: John F. Hess, Ph.D.
Paul G. Fitzgerald
John C. Voss

CONTRACTING ORGANIZATION: University of California
Davis, CA 95616

REPORT DATE: July 2005

TYPE OF REPORT: Final

PREPARED FOR: U.S. Army Medical Research and Materiel Command
Fort Detrick, Maryland 21702-5012

REPORT DOCUMENTATION PAGE

Form Approved
OMB No. 0704-0188

1. REPORT DATE *(DD-MM-YYYY)*	2. REPORT TYPE	3. DATES COVERED *(From - To)*
01-07-2005	Final	15 Jun 2002 – 14 Jun 2005

4. TITLE AND SUBTITLE
Analysis of Keratin Filament Assembly/Disassembly and Structure Following Modification by Sulfur Mustard Analogs

5a. CONTRACT NUMBER

5b. GRANT NUMBER
DAMD17-02-1-0664

5c. PROGRAM ELEMENT NUMBER

6. AUTHOR(S)
John F. Hess, Ph.D.
Paul G. Fitzgerald
John C. Voss

E-mail: jfhess@ucdavis.edu

5d. PROJECT NUMBER

5e. TASK NUMBER

5f. WORK UNIT NUMBER

7. PERFORMING ORGANIZATION NAME(S) AND ADDRESS(ES)
University of California
Davis, CA 95616

8. PERFORMING ORGANIZATION REPORT NUMBER

9. SPONSORING / MONITORING AGENCY NAME(S) AND ADDRESS(ES)
U.S. Army Medical Research and Materiel Command
Fort Detrick, Maryland 21702-5012

10. SPONSOR/MONITOR'S ACRONYM(S)

11. SPONSOR/MONITOR'S REPORT NUMBER(S)

12. DISTRIBUTION / AVAILABILITY STATEMENT
Approved for Public Release; Distribution Unlimited

13. SUPPLEMENTARY NOTES

14. ABSTRACT
Abstract follows.

15. SUBJECT TERMS
No subject terms provided.

16. SECURITY CLASSIFICATION OF:			17. LIMITATION OF ABSTRACT	18. NUMBER OF PAGES	19a. NAME OF RESPONSIBLE PERSON
a. REPORT	b. ABSTRACT	c. THIS PAGE			19b. TELEPHONE NUMBER *(include area code)*
U	U	U	UU	44	

ABSTRACT

The modification of keratin and vimentin intermediate filaments and proteins by the sulfur mustard analogs chloroethyl ethyl sulfide and mechlorethamine has been studied using electron microscopic and electron paramagnetic approaches. The modification of intact filaments leads to abnormalities in the filaments such that native filament appearance is destroyed. Modification of purified proteins, followed by dialysis to assemble native filaments, shows that the modified proteins do not assemble into smooth native looking filaments. In both cases, the appearance in the electron microscope is filamentous, but with much more particulate, irregular aggregations. Comparison of these chemically modified proteins to specific mutations associated with skin blistering diseases reveals difference between the filaments.

Using an electron paramagnetic approach, it has been possible to examine the early stages of normal heteropolymeric keratin filament assembly for characteristics that are related to our findings with the homopolymeric protein vimentin. Thus, we have identified spectral changes that occur during assembly and have further identified amino acid regions in one keratin protein that are in close proximity with another region of the polymerization partner. Subsequently, the assembly of chloroethyl ethyl sulfide and mechlorethamine treated keratins was analyzed, revealing a change in the assembly dynamics but showing evidence of some proper assembly. It is likely that near normal filament assembly occurs at early stages, but additional aberrant interactions are produced as a result of covalent modification.

Table of Contents

Introduction

In the early 1990s, several research groups identified keratins as the entity involved in inherited skin blistering diseases [1-3]. Pathologically, skin blistering in epidermolysis bullosa simplex (EBS) occurs at the basal cell layer [4, 5] and usually involves mutations in keratins k5 or k14 [4] [6], the keratin pair specifically expressed in the basal layer of the epidermis [7]. However, it has been shown that mutations in proteins that associate with keratins can result in skin blistering syndromes with the implication that these mutations lead to keratin filament instability [8-11]. Chemical weapons termed vesicants also lead to skin blistering and the mechanism behind the vesicant action is an active area of research [12-15]. Vessicants have the ability to modify numerous cellular components, including proteins and nucleic acids. My original proposal outlined an *in vitro* approach to test the effect of sulfur mustard analogs on keratin proteins.

My proposal was to examine the modification of keratin proteins by an analog of mustard gas called 2-chloroethyl methanethiosulfonate (CE-MTS). This chemical was chosen for 2 major reasons: 1) CE-MTS modifies proteins at cysteines leaving a chloroethyl group attached to the protein, similar, but not identical to the alkylation produced by mustard gas and 2) I have had success using similar methanethiosulfonate (MTS) compounds to spin label cysteine amino acids within the intermediate filament (IF) vimentin to study IF structure and assembly. My proposal, as written, focused on keratin proteins k5 and k14 the major keratins of the basal layers of the skin. The SM analogs CEES and MEC were also to be tested.

A key component of my proposal was the application of both methods and results obtained from the study of vimentin assembly and structure to the study of keratin structure. As such, experiments were proposed using assembly of vimentin to provide structural information that could be transferred to keratin structure. These experiments have been performed.

A second component of my proposal was the study of an EBS type mutation and the structural consequences of the amino acid substitution on IF structure. This aim has been studied in vimentin preliminary to studies in keratins. A recent publication [16] casts doubt on the generalization that all EBS mutations prevent filament assembly and we have studied this mutant by conventional and EPR methods.

The title of the proposal and the overall goal of the proposal is to study keratin filament structure and assembly after modification with CE-MTS. The preliminary data generated by the study of vimentin and the methods developed to study the effect of the EBS mutation have progressed to the stage where meaningful experiments can be performed on control keratins, keratins modified by CE-MTS and keratins which have been modified and the modification removed. Additional experiments are described that characterize keratin assembly intermediates and these data are used to compare to data derived from CEES and MEC treated keratins. We find that electron microscopy reveals a filamentous character to the non-IF aggregates and EPR can identify similarities between treated and untreated proteins.

Body

1. Effects of SM analogs on keratin IFs

As previously described, the codon optimization of k14 (keratin 14) did not change the expression level of bacterially expressed k14. Due to the amount of relatively pure protein required for filament assembly and other experiments, the decision was made to proceed with bacterial expression of keratins 5, 8 and 18, forgoing k14. Due to the ability of any type I keratin to co-assemble with any type II keratin [17], experiments were planned with k5 (keratin 5) and k18 (keratin 18). In addition, a keratin fraction (major expressed pairs, k1/10 and 5/14) was isolated from bovine snout. Together, the bacterial expressed keratins and bovine isolated keratin provided the materials for characterization of the effects of SM (sulfur mustard) analogs on IF assembly.

Recombinant k8 and k18 were purified to >90% pure as judged by SDS-PAGE (sodium dodecyl sulfate-polyacrylamide gel electrophoresis). Similarly, a keratin pool containing k5/k14 and k1/10, isolated from bovine snout were ~90+% pure (Figure 1). Both bacterially produced and natively isolated keratin pairs formed long, smooth, native-appearing 10 nm filaments as judged by EM (figure 1B and 1C). Exposure of the kIFs (keratin intermediate filaments) to either 1% DMSO (dimethyl sulfoxide) or 1% ethanol solvents induced only very slight changes (DMSO shown in Figure 1D). Increasing either solvent concentration to 10% however, resulted in filament aggregation, similar to treatment with vesicant analogs (Figure 1E). All experiments reported contained a final solvent concentration of 1%.

Keratin filaments produced in vitro and treated with 10 mM CEES (chloroethyl ethylsulfide) or MEC (mechlorethamine) induced dramatic changes to the filaments (figure 2, panel A, B). Figure 2A shows 2 representative views of k8/18 filaments treated with 10 mM CEES. The aggregation of kIFs into irregular species is apparent. After examination of many EM fields, it is not possible to find intact filaments. Figure 2B shows k8/18 filaments after treatment with 10 mM MEC. In panel A, a filamentous character underlies a pattern of roughly spherical particles. Individual filaments are rare, but bundles of filaments are common. In panel B, the bundles of filaments are clearly evident and the production of spherical particles is not as common. Nevertheless, the conclusion is clear: exposure of kIFs to 10 mM CEES or MEC is severely damaging.

Treatment of keratin proteins was also performed followed by dialysis of proteins to assemble filaments. In these experiments, CEES and MEC were added to proteins in 8 M urea and incubated for a limited time. Samples were then dialyzed to assemble filaments. Figure 3A shows native looking filaments assembled from keratin proteins treated with DMSO (solvent control). Figure 3B shows the type of aggregated keratin assemblies produced by 10 mM CEES modified keratins. A filamentous background exists, but numerous larger aggregates also seem to decorate or be part of the filamentous network. Figure

3C shows the aggregated assemblies that result from treatment of keratin proteins with 10 mM MEC. This treatment produces larger particles that seem to be connected by regions of filaments, either native looking filaments or larger bundles. Overall, the particles seem to aggregate, making the visualization of filamentous regions more difficult.

Our results show that treatment of both bacterially produced (k8/18) or natively isolated keratin (k1/10 and 5/14) filaments with CEES and MEC causes large scale protein aggregation with limited evidence of remaining filamentous structure. Treatment of purified keratin proteins followed by dialysis to assemble IFs also produces misshapen aggregates instead of native looking IFs.

Chemical modification of cysteine side chains

A fundamental difference between the keratin pair k8/18 and either of the keratin pairs k5/14 and K1/10 is the presence of several cysteine residues in both k5/14 and 1/10, with none in either k8 or k18. To investigate the sensitivity of keratin assembly to modification of cysteine side chains, we used the sulfhydryl reactive reagent 2-chloroethyl-MTS to modify k5/k14 and k1/k10 cysteines. Treatment of cysteine containing proteins with this reagent results in the modification of the cysteine with the addition of a CE (chloro-ethyl) group. Figure 4 shows a series of electron micrographs depicting the changes to k5/14 and 1/10keratin filaments produced by modification with CE-MTS. Panels A and B shows keratin filaments assembled from CE-MTS modified keratin proteins assembled in the absence of DTT. In A, an EM field chosen to show the most normal looking possibility, the filaments look long and smooth, but there is evidence of aggregation. In panel B, a field chosen to represent a more typical view, protein aggregation decorates a filamentous backbone. Panels A and B are taken from the same EM grid, from the same dialysis reaction and were chosen to indicate heterogeneity seen in the EM.

The modification of proteins with the sulfhydryl specific reagent CE-MTS has the additional advantage of being reversible. Dialysis of modified proteins in the presence of DTT will remove the CE group. As controls for the filament assembly reactions using modified proteins, we analyzed the assembly capability of CE modified proteins in assembly buffer plus DTT. In the presence of DTT, and therefore with all modifications reversed, CE-MTS treated keratins should form long filaments after dialysis (panels C and D). Thus, CE-MTS modification of keratins introduces sufficient change to interfere with normal assembly, but removal of the modification restores the ability of the keratins to assemble.

An additional experiment was performed to determine the ratio of modified proteins to unmodified proteins that would cause filament abnormalities. Figure 5 shows that unmodified keratins produce a thick mass of long keratin filaments (figure 5A). Inclusion of an equal mass of CE-MTS modified keratins produces very few long filaments and yields mainly incomplete filaments with few identifiable normal looking filaments (figure 5B).

Mixing unmodified keratins with CE-MTS modified keratins at a 9:1 ratio, also produces obvious filament abnormalities (figure 5C).

Further characterization of the effects of CE-MTS modification was performed using bacterially expressed and purified mutants of k5, each containing different numbers of cysteine amino acids. In these experiments, the cysteine codons of k5 were changed to serine and the following combinations examined: 1) cys head, ser tail (cys^{55}, cys^{135}, ser^{407}, ser^{479})

2) ser head, cys tail (ser^{55},ser^{135}, cys^{407}, cys^{479})

3) cys minus (ser^{55},ser^{135}, ser^{407}, ser^{479}).

The bacterially produced keratins were CE-MTS treated using the same procedure as for bovine isolated keratins. Figure 6 shows the results of these experiments. Panel A and panel B of figure 6 show filaments assembled from CE-MTS modified cys head and cys tail, respectively. These proteins each contain cysteines at the wild type location in the head and tail, respectively, and form normal looking IFs when viewed in the EM. Panel C is a sample of wild type k5 containing the normal complement of 4 cysteine amino acids; it too forms IFs when examined in the EM. The filaments appear, subjectively, slightly different from wild type, but the conclusion is that CE modification of wild type K5 is compatible with filament assembly. Panel D is a negative control, a cysteine minus k5 mutant (ser^{55},ser^{135}, ser^{407} and ser^{479}) unable to be modified by CE-MTS is treated and purified exactly as the other samples. This cysteine minus mutant is as expected, fully able to form IFs.

Assembly of the CE-MTS modified keratin 5 proteins was also performed in the presence of DTT, which should remove the CE modification. In these conditions, all the proteins formed IFs, as expected (data not shown).

Discussion

Since the first demonstrations that native looking IFs could be assembled from purified proteins, IF biology has been replete with reports of the importance of whole regions or individual amino acids for assembly of native filaments (for reviews, see [4, 18, 19]; for an example of exhaustive mutagenesis see,[20]. The final verification of this research was the understanding that single amino acid substitutions within keratin genes were the cause of inherited skin blistering diseases [1, 3, 21]. Thus, a concordance between in vitro experiments and the locations of EBS causing mutations revealed the sensitivity of IF structure and function to single amino acid changes [22-24]. As expected from mutagenesis experiments, two highly conserved domains, the helix initiation and helix termination domains, are hotspots for disease causing mutations.

On the opposite end of the protein structure/function equation is the generalized modification of cellular proteins by agents such as mustard gas. At the cellular level, mustard gas exposure produces bulla (blisters) between the dermis and epidermis [25] and thus superficially resembles the location of bulla in EBS [21]. Our experiments are directed at the possibility that the "non-specific" modification of keratin proteins and filaments by mustard gas analogs

can damage the filaments, resulting in collapse of the filament network, leading to cell lysis. Such a possibility would extend the similarity between chemical vesicants and EBS. In contrast to the specificity of a single amino acid change, chemical modification produces changes at many places and it is possible that protein modification is highly variable, both within a single protein molecule and between protein molecules in a filament.

Using analogs of mustard gas, our data show that significant damage to keratin filaments occurs following exposure to either 10mM CEES or MEC. In the assembled filament, exposure to CEES or MEC results in filament destruction through what appears to be an aggregation phenomena. In the EM, chemically treated keratin filaments appear as thickened filaments with extra particles. Underlying the sample's appearance is a filamentous character, but not native looking 10 nm filaments, a much larger diameter rope type filament. The source of the particles, whether locally unraveled filaments that aggregate into a mass, or aggregated remains of different filaments is unknown. Treatment with CEES produces more aggregation than an equimolar amount of MEC or alternatively, MEC treated filaments appear more filamentous than CEES treated filaments. If the modification of kIFs is a highly variable process, then damage to kIFs can be viewed as a continuum of protein subunits on the outside of the filament being more heavily modified than protein molecules located on the interior of the filament. Longer treatments or higher concentrations of agent can be expected to modify existing filaments to a greater degree. This variable modification of existing filaments could underlie the filamentous character of CEES and MEC treated kIFs; modified proteins on the surface of the protein aggregate together while the relatively unmodified central proteins contribute to a filamentous structure.

The specific, limited and reversible modification of keratins using CE-MTS reveals that relatively few modifications can interfere with proper filament assembly. Keratin 5 and k14 each contain 4 cysteine residues, 2 each in the head and tail domains. We have modified these positions with a chloroethyl group using a methylthiosulfonate cysteine specific reagent. Keratin proteins modified by this reagent are incapable of assembling into native looking filaments. Furthermore, incorporation of modified proteins at a 10% level is enough to produce visible abnormalities to keratin assembly. These results are consistent with experiments published by Steinert and Parry who found that modification of keratin 1 or 10 by iodoacetate prevented filament assembly [26]. In these experiments, modified keratins were either mixed together or mixed with native assembly partners, no attempt was made to mix different proportions of modified proteins. Our experiments show that a relatively minor proportion of modified proteins has a noticeable effect on filament assembly.

These experiments demonstrate that modification of keratin protein molecules either assembled into filaments, or individually in solution, is detrimental to keratin intermediate filaments. While these data were obtained in vitro, is they are consistent with limited experiments demonstrating a similar

effect using iodoacetate and the generality that chemical modification of keratins should interfere with assembly. It is likely that modification of keratins in vivo is equally damaging, but whether or not modification of keratins proper or some other intermediate filament associated protein results in the blistering produced by sulfur mustard is unknown. Our experiments leave open the possibility that modification of keratins is a key component of vesicant induced blistering.

2. EPR analysis of keratin assembly

In a previous report, I described preliminary data that indicated the alignment of the kIF coiled coil within rod 2B was perhaps out of register by 2 amino acids. Those data will not be repeated here, and additional set of spectra from rod domain 1B are not yet completed. For these experiments, k8 position 163 (predicted to be an "a" position of the heptad repeat) was mutated to a cysteine and spin labeled. Adjacent to k8 position 163 is predicted to be k18 position 135. Mutants were designed for k18 positions 131-138 and proteins produced and spin labeled for mixing experiments. As with results presented for rod 2B previously, the best experimental course to be pursued in the future is the construction of mutants in k8 AND k18 over a 1-2 heptad region followed by the mixing of each mutant with all the others (type I keratins with type II) and spectra collected.

The previous experiments were designed to verify coiled coil structure within rod domain 1B, which would be verify long untested predictions of keratin structure [27, 28] and would be consistent with our previous EPR (electron paramagnetic resonance) characterization of vimentin. However, higher order assemblies of keratin proteins can also be probed by an EPR approach. This has been ably demonstrated by our experiments with vimentin [29-31] and has been investigated in keratins with an identical approach.

The fundamental building block of vimentin filaments is a homodimer of 2 individual protein molecules. The fundamental building block of keratin filaments is a heterodimer of 1 type I keratin with 1 type II keratin [32, 33]. In both cases, assembly of the dimer proceeds next to a tetramer, then to an octamer, and subsequently to not-well-characterized "protofilaments" or "unit length" filaments, followed by elongation into full length filaments. Using and SDSL-EPR (site directed spin labeling-electron maramagnetic resonance) approach we have determined that vimentin assembly proceeds first to an A_{11} dimer (meaning an A_{11} structure is present, but no A_{22} structure is present) and then to a structure (hexamer or octamer) with an A_{11} and A_{22} alignment [30]. We have investigated the assembly of keratin subunits using the same strategy.

Based on our results with vimentin and from crosslinking studies performed by Steinert and co-workers [34] we predicted structure A_{11} should involve k8 positions 189-203 lying in close proximity to K18 positions 161-171. Keratin 8 positions 189, 192, 196, 199, and 203 are predicted to be "non a,d" heptad positions and thus, their side chains, when mutated to cysteine and spin

labeled, will lie on the outside of the coiled coil. Similarly, k18 positions 161, 165, 168, and 171 represent exterior of the coiled coil positions. Each of these mutants was constructed, prepared, purified and spin labeled. Figures 7-10 show the spectra from numerous of these mixing experiments. The key spectra are from samples labeled at k8 position 196 and k18 position 165 and 168 (figure 8 and 9). Spectra from k8 position 196 demonstrates an interaction with k18 positions 165 and 168, seen as an almost identical line shape for the 4M and 2M urea spectra. Using vimentin experiments as a guide, the spectra are interpreted as follows. In 8M urea, the keratin chains are denatured and the spectra from each spin label is tall and narrow indicating no defined protein structure. As the urea concentration is lowered to 6M, keratin chains assemble and the rotational freedom of the chains is decreased. This reduction in spin label freedom also occurs with subsequent lowering of the urea concentration, indicating a smooth assembly and attainment of structure. The spectra of keratin mixtures K8 189 spin mixed with k18 161 spin shows the gradual process. Note the rightmost signal; blue, green red and black spectra are not overlapped at the peaks, their amplitudes are different and decrease from 8M to 2M urea.

However, the spectra for k8 196 mixed with k18 168 (figure 9) shows nearly identical spectra at 4M and 2M urea concentrations (see also figure 8, k8 196 mixed with k18 165). The interpretation for this result is the interaction of spins on the 2 separate polypeptide chains produces the observed spectra and the interaction is the same at the 2 concentrations of urea. Thus, keratins in 4M urea have formed the A_{11} structure and an interaction between k8 196 and k18 168 spin labels is revealed. In 2 M urea, additional protein assembly may take place, but the interaction between k8 196 and k18 168 remains in place and the spectra look nearly identical. Ultimately, as assembly produces filaments, with extensive protein-protein interaction, the EPR spectra will reveal an even more rigid, spin-spin interacting spectra. Within figure 9, the spectra of k18 168 spin mixed with k18 192, 199 and 203 all show normal adoption of structure, different from the k18 196 spectra. The spectra of k18 168 spin mixed with k8 189 shows a broad spectrum (generally speaking, flattened) indicating a very rigid structure. This is different from the spin-spin interaction revealed by the k18 168 k8 196 mix.

Investigation of figure 8 reveals evidence for interactions between k8 196 and k18 165. In this situation however, the 4M and 2M are not as identical as for k18 168 and k8 196, indicating that the 2M spectra, due to packing of protein chains brings the spin labels closer together than they are in 4M urea.

EPR investigation of the A_{22} structure of keratins was performed in an analogous fashion, using k8 and k18 proteins spin labeled in rod 2B. K8 was spin labeled at positions 351, 353 and 357. K18 was spin labeled at positions 320, 323, 325, 327 and 331. The mixing experiments are grouped by spin labeled k8 position and presented as figures 11-13, k8 351, 353 and 357 respectively. Spectra from mixtures of k8 351 and all the spin labeled k18 samples show an orderly adoption of structure, with no significant evidence of spin-spin interaction (figure 11). Spectra from position spin labeled k8 353 (figure 12) show evidence

of spin-spin interaction between k8 353 and k18 323, indicative of the A_{22} structure. This is seen by examination of the almost perfect overlap between the 4M and 2M spectra (figure 12). A very similar result is seen in figure 13, as a result of mixing spin labeled k8 357 and k18 spin labeled 323.

EPR analysis of an EBS-like mutant

One of the first EBS mutants to be identified was the change of k14 amino acid 125 from arginine to cysteine [21]. This change was identified in patients with EBS and was demonstrated to cause a skin blistering disease in transgenic mice. The effect of this mutant of this change on IF assembly was assayed both in vitro and in tissue culture cells by transfection of mutant and control constructs [21] and in both cases, found to exhibit defects. The only reason to doubt the conclusions from these experiments was the inclusion of an antibody recognition epitope at the carboxy tail of the construct to enable the differentiation of the transiently expressed protein from the wild type protein. This tag was added to the wild type k14 construct and found not to interfere with assembly in vitro or in transfected tissue culture cells. However, in 2002, Herrmann et al. reported that the similar EBS causing (and believed to be functionally identical) mutant of k14 arg^{125}->his^{125} was better at filament assembly in vitro than the wild type protein [16]. Thus, the generalization that EBS mutation equals impaired filament assembly has been called into question.

Using vimentin as a model system, we began EBS characterization with a vimentin LNDC or LNDS mutant of the wild type helix initiation sequence LNDR. These studies were published in JBC in 2005 [29] (Appendix).

We extended this methodology to keratins, by investigating the keratin 8 and 18 mutants LNDC. These studies were performed in collaboration with Paul FitzGerald and Josh Pittenger (UC Davis). Keratin 18 LNDC assembles into filaments, but with not as avidly as wild type k18 (figure 14, panel B). K8 LNDC is much more impaired in filament assembly (figure 14, panel C). Some normal looking filaments are present, but these are found in aggregates, against a background of particles. A normal appearing pattern of long filaments on in an EM field does not occur. The mixture of k8 LNDC and k18 LNDC, which should be functionally identical to a vimentin LNDC mutant (figure 14, panel D), does not produce any normal looking filaments.

Examination of the EPR spectra of assembly intermediates reveals that the LNDC mutant either assembles or aggregates more rapidly than the wild type proteins (Figures 15 and 16). This is revealed by a comparison of the spectra recorded in 6M and 4M urea. The spectra from the k18 LNDC mutant show a lower amplitude, indicating more rigid structure. In figure 15, the mutant protein is k18 and the spin labeled protein is k8. In figure 16, the mutant protein is k8 and the spin labeled protein is k18. From these experiments, the EPR spectra reveal a greater change to filament assembly dynamics when the LNDC is present in the k8 protein. A similar result is seen in the EM, following a complete dialysis protocol to assemble kIFs. In the EM, k8 LNDC assembles

poorly, forming mainly short rods while k18 LNDC assembles into numerous filaments (figure 14).

As shown by EPR and electron microscopy, the k8 LNDC mutant has a greater impact on assembly. Viewed in the EM, the only possible interpretation is that k8 LNDC effects filament elongation, but the structure of assembly intermediates is not know. One possible interpretation of the EPR spectra of figure 16 is that the LNDC mutant produces either a k8/k8 aggregation or a k8/18 aggregation with appreciable protein-protein contacts. K8 LNDC spectra from samples in 2 and 4M urea are much more broadened (flatter) than the corresponding native samples. Thus, the EPR approach reveals that at the earliest stages of assembly, the LNDC mutants are not normal.

EPR analysis of CEES or MEC treated keratin assembly

An electron microscopy approach provided evidence that treatment of kIFs with the SM analogs CEES or MEC damaged intact filaments and that similar treatment of soluble keratin monomers prevented normal assembly of filaments. Further characterization of modified keratin proteins showed that modification of cysteines could interfere with filament assembly, but only if both assembly partners were modified. However, the electron microscopy approached limited the analysis of the effects of CEES and MEC on filament assembly. With the characterization of keratin assembly by EPR spectra preliminarily completed, it became possible to analyze the effects of protein modification on early steps of filaments assembly.

For this series of experiments, spin labeled keratins in 8M urea were mixed, divided into three samples and then incubated alone or with either CEES or MEC. Each keratin sample was then dialyzed against 8M urea to remove the CEES or MEC. Each sample was then diluted in a step wise fashion, with an hour incubation at each step, from 8M to 6M, to 4M and finally 2M urea. Spectra were then recorded and signals normalized based on dilution. To assess the formation of an A_{11} structure, k8 spin 196 and k18 spin 168 were mixed. To assess the formation of the A_{22} structure, k8 357 spin and k18 323 spin were mixed.

Previous experiments identified the A_{11} tetramer by spin-spin interactions of k8 196 and k18 168, resulting in nearly identical spectra at 4M and 2M urea concentrations. Therefore, spectra were collected from samples treated with CEES or MEC in parallel to an untreated sample in urea concentrations ranging from 8M to 2M. The control sample, far left, figure 17, shows a series of spectra that are nearly identical to those shown in figure 9, thus the additional manipulations did not effect the assembly. Figure 17, middle and right show EPR spectra from samples treated with CEES and MEC. The CEES samples show an assembly pattern that is slightly different from the control spectra. The spectra from CEES treated keratins incubated in 6M urea is possibly more ordered than the control spectra, but the spectra from 4M and 2M conditions reveal a difference that is not evident in the control. Compare the red (4M urea) and black (2M urea) spectra; the CEES and MEC treated samples have a sharper

4 M spectra but relatively the same 2M spectra as the control. The easiest interpretation for this result is an interference with the formation of the A_{11} structure. However, the A_{11} structure is not eliminated, it still forms. The CEES and MEC analogs reduce the urea concentration at which the interaction occurs, and thus can be further interpreted as decreasing the strength of the interaction leading to the A_{11} structure. Nevertheless, as judged by the EPR spectra, the A_{11} structure can be seen to form.

The alternate keratin tetramer, A_{22}, formed by overlap of the rod 2B between dimers, was examined by mixing k8 357 spin and k18 323 spin. Figure 18 shows a series of EPR spectra from samples treated exactly as described above for the A_{11} structure. Similar to the description of the A_{11} results, the EPR characterization of the A_{22} spin-spin interaction reveals that CEES or MEC modification of keratins produces alterations to the spectra thus revealing differences between the assembly of modified proteins and the control.

The experiments describing A_{11} and A_{22} interactions and the interpretation of changes to the spectra by protein modification are difficult to interpret. While the spectra are not identical between controls and treated samples, the modeling of molecular processes and the interpretation of such processes with regard to the model are not sufficiently developed to account for the wide variety of events that could be occurring. For example, proportions of molecules interacting in normal assembly can be determined with the reasonable assumption that assembly is regular and interactions occur regularly (ie, an A_{11} interaction places 50% of the spin labels in an interaction possible position). Covalently modified proteins could produce interactions that are not regular, and that disturb these proportions, and at later stages, could even produce new interactions. Thus, it is important to well characterize normal assembly first, then modified protein assembly. As the structure of very few assembly intermediates has been identified, SDSL-EPR must first be used to identify landmarks, then build on these land marks. We have identified A_{11} and A_{22} structures, but now must move on to A_{12} and possibly A_{cn}

During keratin assembly, formation of the A_{11} and/or A_{22} tetramer has been hypothesized to occur at the same time and result in equilibrium between all the species [35]. Our data from vimentin indicates that the A_{11} tetramer forms at a higher urea concentration, and thus, during dialysis to form filaments, must form before an A_{22} tetramer. This indicates that the A_{11} tetramer is more stable (or alternatively a greater interaction force exists between rod 1B domains) than the A_{22} tetramer in vimentin. Our experiments have not resolved the assembly process in keratins, but it is anticipated that future experiments will identify which keratin structure forms earlier, A_{11} or A_{22}.

The use EM shows that modified keratins retain a degree of filamentous character within the definitely non-native structure shown in figures 2-6. SDSL-EPR characterization reveals that the early stages of keratin assembly are not that disrupted; the early stages are not completely normal, but the presence of particular interactions (A_{11} and A_{22}) shows that at these early stages of assembly,

analogs of SM do not completely eliminate native interactions. It is now possible to propose that CEES and MEC modified proteins for additional non-specific interactions that produce the irregular species seen in the EM. Thus, the next step of analysis is to characterize subsequent stages of filament assembly, beginning with the homopolymeric protein vimentin, and usning the data derived from it, to transition to keratins and then the study of modified proteins can be compared to normal assembly.

Materials and Methods

CEES and MEC were purchased from Aldrich and stored at room temperature. Prior to use, each was prepared as a 1 M stock solution in DMSO (Aldrich). Working dilutions of CEES and MEC were either the 1 M stock or a 100 mM stock prepared in DMSO. cDNA clones for human K8 and K18 were provided by Bishr Omary (Stanford University, Palo Alto, CA). K8 and K18 cDNA sequences were inserted into pT7-7 for bacterial expression [36]. Bacterially expressed K8 or K18 readily formed inclusion bodies and these were purified from bacterial cell pellets [31, 37] Inclusion bodies were dissolved in buffer A (10 mM Tris, pH 8.0, 1 mM EDTA) plus 8 M urea and purified by gel filtration using a Pharmacia FPLC system. Native bovine keratins 5/14 and 1/10 were purified from bovine snout using a protocol provided by Roy Quinlan (University of Durham, UK). Proteins were quantified by BCA assay (Pierce, Rockford, IL) and proteins stored at -80°C.

Treatment of filaments or purified proteins was performed by adding 1 microliter of the stock CEES or MEC (1M or 100mM) reagent solution to 99 microliters of protein solution. Solvent controls were performed analogously. Treatments were performed in a laboratory fume hood and incubated for the indicated times. After incubation, samples were spotted onto EM grids and processed normally; following drying, the grids were removed from the hood. Electron microscopy was performed as described by Quinlan and coworkers [38].

Chloroethyl-MTS treatment of k5/14 and 1/10 was performed by treating proteins with 100 mM TCEP to reduce cysteines followed by incubation with CE-MTS (500 mM CE-MTS final concentration). Control samples were incubated with solvent alone. Following a 1 hour treatment, samples were dialyzed against filament assembly buffers either containing (+DTT) or without DTT (-DTT).

Filaments were assembled using a multistep dialysis method. Purified keratin subunits in 8 M urea buffer were mixed, placed into dialysis tubing and dialyzed against fresh buffer A plus 8 M urea (1 hours), followed by buffer A plus 4M urea (2 hours), then 10 mM Tris pH 8.0 (2 hours), 10 mM tris pH 7.0, 1 mM $MgCl_2$ (2 hours), and finally, 10 mM Tris pH 7.0, 1 mM $MgCl_2$, 50 mM NaCl (overnight). During the course of these experiments, an abbreviated process was also developed: 1 hr in buffer A plus 8 M urea, 1 hr in buffer A plus 4 M urea, then 1 hour in 10 mM tris pH 7.5, followed by overnight dialysis in 10 mM tris pH 7.5, 1 mM $MgCl_2$, 50 mM NaCl. Filaments formed by either method were indistinguishable.

Mutants were prepared using the Stratagene Quickchange kit (Stratagene, La Jolla, CA) and oligonucleotide primers purchased from Invitrogen (Invitrogen, Carlsbad, CA). DNA sequencing was performed by Davis Sequencing (Davis, CA) to verify successful mutagenesis. Proteins were produced by bacterial expression using a pT7-7 vector [36] and BL21 (DE3) codon optimized or arabinose inducible cells (Codon optimized cells from Stratagene, La Jolla, CA; arabinose inducible from Invitrogen, Carlsbad, CA). intermediate filament proteins readily form inclusion bodies and these were purified using a lysozyme lysis/DNase I treatment followed by high and low salt washes [31, 37]. Spin labeling of purified proteins was as described in recent papers [29-31].

Analysis of keratin mixtures was performed by mixing equimolar amounts of keratin in 8M urea followed by either dialysis against the indicated concentrations of urea or step-wise dilution of samples along 8-6-4-2M urea steps, with one hour at each urea concentration prior to dilution. Control keratin partners were the normal wild type sequence unless otherwise noted.

EPR measurements were carried out in a JEOL X-band spectrometer fitted with a loop-gap resonator [39]. An aliquot of purified, spin-labeled protein (5 mL) at a final concentration of ca. 100 mM protein was placed in a sealed quartz capillary contained in the resonator. Spectra of samples at room temperature (20-22 ^{0}C) were obtained by a single 60 sec scan over 100G at a microwave power of 2 mW and a modulation amplitude optimized to the natural line width of 1G, as described previously [40].

Key Research Accomplishments

This project has introduced a new technique to the study of intermediate filament structure and assembly: SDSL-EPR (Site Directed Spin labeling and Electron Paramagnetic Resonance). Although the technique is not new to the study of membrane proteins, it is new to the study of filamentous proteins such as intermediate filaments. As with the introduction of any new technique, the validation of the method and the performance of controls are essential to future progress. Thus, we have undertaken the study of the homopolymeric protein vimentin as a precursor to the study of heteropolymeric keratins. This "start with vimentin, then switch to keratins" approach was written into the original proposal, but not envisioned to take as long as it did. As such, progress on the keratin modification, assembly and disassembly was slow to begin. It is however well underway and many accomplishments have been made.

•Vimentin assembly intermediates were identified and published [17](described in a previous report) and this approach has been performed with keratins (this report).

•A vimentin mutation analogous to an EBS mutation has been studied by EM and EPR [16]; this methodology has been followed with keratin mutants (this report).

•Keratin assembly has been characterized by EPR of individual amino acids within rod domains and interactions between keratin protein domains has been identified by EPR (this report).

•Conditions have been identified that are compatible with protein structure determination and EPR (ie, full length filaments are not possible to efficiently load into capillaries, so different buffers conditions are used).

•Keratin proteins and filaments have been modified with 3 different reagents and the effects on filaments studied by EM and EPR (this report).

•Demonstrated that mixtures of non-native keratins and keratin mutants can provide structural data (ie, mixing k5 with k18 and k5 mutants with k18).

Reportable Outcomes

The data contained in this report should form the basis for 3 manuscripts. First, a paper the effects of CEES and MEC on keratin filaments and keratin proteins has been written and should be submitted in the very near future. This manuscript will not present any EPR data, but will demonstrate the effects of protein modification on both filaments and filament assembly. This manuscript leaves open the possibility that SM modification of intermediate filaments could be responsible for skin blistering. The degree of modification required to achieve filament abnormalities could explain the time lag between exposure and skin blistering.

Second, a manuscript describing the normal assembly of keratin proteins into filaments as monitored by EPR will be prepared. This manuscript will contain a characterization of rod domain 1B and 2B coiled coil assembly as well as the identification of A_{11} and A_{22} interactions. It is likely that this paper will also contain our characterization of the effects of an EBS like mutation on assembly.

Third, the effects of SM analogs on keratin filament assembly will be documented and compared to the data presented in manuscript 2. This manuscript will present EPR data and an analysis of assembly using an EPR approach.

Conclusions

The main conclusion for this avenue of research is that SDSL-EPR provides a powerful, albeit labor intensive, method to identify Intermediate Filament structure. Experiments can be designed that add detail to existing outlines of filament structure. Validation of experiments using a homopolymeric system are an essential staring point; control experiments using a single keratin molecule are uninformative (ie, using one keratin and not a pair of keratins in an assembly reaction). The information provided by EPR of vimentin has already provided new information for the characterization of an EBS-like mutation and those experiments have been transferred to the analysis of a keratin mutant. Thus, this approach provides a valuable method for determining the structure and assembly of both vimentin and keratin filaments.

In addition, this approach enables the study of filament assembly and disassembly induced by chemical modification. We have determined that the SM analogs CEES and MEC are compatible with the specific spin labels used and that downstream procedures can be used with very little modification. The study of assembly of IFs is at the present time, much more valuable than the study of disassembly due to the inherent lack of specificity of an individual spectrum (ie, the spectrum of an irregular aggregation of proteins can resemble the spectrum of an assembled filament, indicating protein-protein contacts and rigid conformation. Unfortunately, it can all be an artifact). The study of assembly and the characterization of normal interactions thus provides a framework upon which to test the chemically modified proteins. Ultimately, with a sufficient number of markers identified, SM analog disassembly can be approached.

References

1. Bonifas, J.M., A.L. Rothman, and E.H. Epstein, Jr., Epidermolysis bullosa simplex: evidence in two families for keratin gene abnormalities [see comments]. Science, 1991. 254(5035): p. 1202-5.
2. Coulombe, P.A., et al., A function for keratins and a common thread among different types of epidermolysis bullosa simplex diseases. Journal of Cell Biology, 1991. 115(6): p. 1661-74.
3. Lane, E.B., et al., A mutation in the conserved helix termination peptide of keratin 5 in hereditary skin blistering. Nature, 1992. 356(6366): p. 244-6.
4. Fuchs, E. and K. Weber, Intermediate filaments: structure, dynamics, function, and disease. Annual Review of Biochemistry, 1994. 63(1): p. 345-82.
5. Fine, J.D., et al., Revised clinical and laboratory criteria for subtypes of inherited epidermolysis bullosa. A consensus report by the Subcommittee on Diagnosis and Classification of the National Epidermolysis Bullosa Registry. J Am Acad Dermatol, 1991. 24(1): p. 119-35.
6. Fine, J.D., et al., Revised classification system for inherited epidermolysis bullosa: Report of the Second International Consensus Meeting on diagnosis and classification of epidermolysis bullosa. Journal of the American Academy of Dermatology, 2000. 42(6): p. 1051-66.
7. O'Guin, W.M., et al., Differentiation-specific expression of keratin pairs, in Cellular and molecular biology of intermediate filaments, R.D. Goldman and P.M. Steinert, Editors. 1990, Plenum: New York. p. 301-334.
8. Banwell, B.L., et al., Myopathy, myasthenic syndrome, and epidermolysis bullosa simplex due to plectin deficiency. Journal of Neuropathology and Experimental Neurology, 1999. 58(8): p. 832-46.
9. McLean, W.H., et al., Loss of plectin causes epidermolysis bullosa with muscular dystrophy: cDNA cloning and genomic organization. Genes and Development, 1996. 10(14): p. 1724-35.
10. Wiche, G., Role of plectin in cytoskeleton organization and dynamics. J Cell Sci, 1998. 111 (Pt 17): p. 2477-86.
11. Kunz, M., et al., Mutation reports: epidermolysis bullosa simplex associated with severe mucous membrane involvement and novel mutations in the plectin gene. J Invest Dermatol, 2000. 114(2): p. 376-80.
12. Chakrabarti, A.K. and P. Ray, Novel endogenous inhibitor of sulfur mustard-stimulated protease in cultured human epidermal keratinocytes: possible application in vesicant intervention. Journal of Applied Toxicology, 2000. 20 Suppl 1(5): p. S59-61.
13. Monteiro-Riviere, N.A. and A.O. Inman, Ultrastructural characterization of sulfur mustard-induced vesication in isolated perfused porcine skin. Microscopy Research and Technique, 1997. 37(3): p. 229-41.
14. Werrlein, R.J. and J.S. Madren-Whalley, Multiphoton microscopy: an optical approach to understanding and resolving sulfur mustard lesions. J Biomed Opt, 2003. 8(3): p. 396-409.
15. Dillman, J.F., 3rd, K.L. McGary, and J.J. Schlager, Sulfur mustard induces the formation of keratin aggregates in human epidermal keratinocytes. Toxicol Appl Pharmacol, 2003. 193(2): p. 228-36.

16. Herrmann, H., et al., Characterization of early assembly intermediates of recombinant human keratins. J Struct Biol, 2002. 137(1-2): p. 82-96.
17. Hatzfeld, M. and W.W. Franke, Pair formation and promiscuity of cytokeratins: formation in vitro of heterotypic complexes and intermediate-sized filaments by homologous and heterologous recombinations of purified polypeptides. Journal of Cell Biology, 1985. 101(5 Pt 1): p. 1826-41.
18. Goldman, R.D. and P.M. Steinert, Cellular and Molecular Biology of Intermediate Filaments. 1990, New York, NY: Plenum Press.
19. Parry, D.A. and P.M. Steinert, Intermediate filaments: molecular architecture, assembly, dynamics and polymorphism. Q Rev Biophys, 1999. 32(2): p. 99-187.
20. Wu, K.C., et al., Coiled-coil trigger motifs in the 1B and 2B rod domain segments are required for the stability of keratin intermediate filaments. Mol Biol Cell, 2000. 11(10): p. 3539-58.
21. Coulombe, P.A., et al., Point mutations in human keratin 14 genes of epidermolysis bullosa simplex patients: genetic and functional analyses. Cell, 1991. 66(6): p. 1301-11.
22. Letai, A., P.A. Coulombe, and E. Fuchs, Do the ends justify the mean? Proline mutations at the ends of the keratin coiled-coil rod segment are more disruptive than internal mutations. Journal of Cell Biology, 1992. 116(5): p. 1181-95.
23. Wawersik, M., et al., A proline residue in the alpha-helical rod domain of type I keratin 16 destabilizes keratin heterotetramers. Journal of Biological Chemistry, 1997. 272(51): p. 32557-65.
24. Fuchs, E. and D.W. Cleveland, A structural scaffolding of intermediate filaments in health and disease. Science, 1998. 279(5350): p. 514-9.
25. Smith, W.J. and M.A. Dunn, Medical defense against blistering chemical warfare agents. Archives of Dermatology, 1991. 127(8): p. 1207-13.
26. Steinert, P.M. and D.A. Parry, The conserved H1 domain of the type II keratin 1 chain plays an essential role in the alignment of nearest neighbor molecules in mouse and human keratin 1/keratin 10 intermediate filaments at the two- to four-molecule level of structure. Journal of Biological Chemistry, 1993. 268(4): p. 2878-87.
27. Hanukoglu, I. and E. Fuchs, The cDNA sequence of a Type II cytoskeletal keratin reveals constant and variable structural domains among keratins. Cell, 1983. 33(3): p. 915-24.
28. Conway, J.F. and D.A.D. Parry, Intermediate filament structure: 3. Analysis of sequence homologies. Int. J. Biol. macromol., 1988. 10: p. 79-98.
29. Hess, J.F., et al., Characterization of Structural Changes in Vimentin Bearing an Epidermolysis Bullosa Simplex-like Mutation Using Site-directed Spin Labeling and Electron Paramagnetic Resonance. J Biol Chem, 2005. 280(3): p. 2141-6.
30. Hess, J.F., et al., Structural Characterization of Human Vimentin Rod 1 and the Sequencing of Assembly Steps in Intermediate Filament Formation in Vitro Using Site-directed Spin Labeling and Electron Paramagnetic Resonance. J Biol Chem, 2004. 279(43): p. 44841-6.

31. Hess, J.F., J.C. Voss, and P.G. FitzGerald, Real-time observation of coiled-coil domains and subunit assembly in intermediate filaments. J Biol Chem, 2002. 277(38): p. 35516-22.
32. Coulombe, P.A. and E. Fuchs, Elucidating the early stages of keratin filament assembly. Journal of Cell Biology, 1990. 111(1): p. 153-69.
33. Hatzfeld, M. and K. Weber, The coiled coil of in vitro assembled keratin filaments is a heterodimer of type I and II keratins: use of site-specific mutagenesis and recombinant protein expression. Journal of Cell Biology, 1990. 110(4): p. 1199-210.
34. Steinert, P.M., et al., Keratin intermediate filament structure. Crosslinking studies yield quantitative information on molecular dimensions and mechanism of assembly. Journal of Molecular Biology, 1993. 230(2): p. 436-52.
35. Mehrani, T., et al., Residues in the 1A rod domain segment and the linker L2 are required for stabilizing the A11 molecular alignment mode in keratin intermediate filaments. J Biol Chem, 2001. 276(3): p. 2088-97.
36. Tabor, S. and C.C. Richardson, A bacteriophage T7 RNA polymerase/promoter system for controlled exclusive expression of specific genes. Proc Natl Acad Sci U S A, 1985. 82(4): p. 1074-8.
37. Nagai, K. and H.C. Thøgersen, Synthesis and sequence-specific proteolysis of hybrid proteins produced in Escherichia coli. Methods in Enzymology, 1987. 153(2): p. 461-81.
38. Carter, J.M., A.M. Hutcheson, and R.A. Quinlan, In vitro studies on the assembly properties of the lens proteins CP49, CP115: coassembly with alpha-crystallin but not with vimentin. Experimental Eye Research, 1995. 60(2): p. 181-92.
39. Hubbell, W.L., W. Froncisz, and J.S. Hyde, A loop gap resonator. Rev. Sci. Instrum., 1987. 58: p. 1879-1886.
40. Chomiki, N., J.C. Voss, and C.H. Warden, Structure-function relationships in UCP1, UCP2 and chimeras: EPR analysis and retinoic acid activation of UCP2. Eur J Biochem, 2001. 268(4): p. 903-13.

Figure Legends

Figure 1. Assembly of purified keratins.

Keratins 8 and 18 were prepared using bacterial expression and purified by chromatography. A mixture of keratins 1/10 and 5/14 was isolated from bovine snout. Panel A shows a Coomassie blue stained SDS gel. Lane 1, purified keratin 8. Lane 2, purified keratin 18. Land 3, bovine snout keratin preparation. Lane M shows Invitrogen Benchmark protein standards, with sizes of appropriate bands indicated on the right. Panel B shows an electron microscope (EM) view of negatively stained k8/18 filaments assembled from purified protein shown in panel A. Panel C shows a similar EM view of assembled bovine snout keratins. Panel D shows an EM view of k8/18 keratin filaments in the presence of 1% DMSO. Panel E shows k8/18 filaments after exposure to 10% DMSO. Scale bar located in the bottom of each panel represents 200 nm.

Figure 2. Treatment of intact IFs with CEES or MEC.

Keratin filaments assembled from k8 and k18 were incubated with 10 mM CEES, panel A, or 10 mM MEC, panel B, and then prepared for electron microscopy. Scale bar located in the bottom of each panel represents 200 nm.

Figure 3. Modification of keratin proteins followed by IF assembly.

Keratins 8 and 18 were mixed together and then incubated with the indicated concentrations of CEES (panel B) or MEC for one hour, followed by dialysis against standard buffers to assemble filaments. Panel A shows a solvent control, 1% DMSO. Panels B and C show CEES and MEC treatment, respectively. The scale bar located in the bottom of each panel represents 200 nm.

Figure 4. Sulfhydryl modification of bovine keratins.

A keratin pool of k1/10 and 5/14, isolated from bovine snout, were treated with the sulfhydryl specific reagent CE-MTS. Panel A shows an EM view of nearly normal IFs seen rarely within the treated samples. Panel B shows a more representative view of the EM view of assembled filaments after treatment with CE-MTS. Panels C and D show representative views of keratin IFs assembled in the presence of DTT from proteins that were modified by CE-MTS. The scale bar located in the bottom of each panel represents 200 nm.

Figure 5. Mixing of modified keratins with unmodified keratins.

Bovine snout keratins were modified by CE-MTS and subsequently mixed with unmodified proteins in various rations. Panel A is the unmodified protein control, all of the keratins are unmodified. Panel B is a 50:50 mixture of unmodified and CE-MTS modified keratins. Panel C is a 90:10 mixture of unmodified keratins to modified keratins, respectively. The scale bar located in the bottom of each panel represents 200 nm.

Figure 6. CE-MTS modification of k5 mutants.

K5 mutants with cysteines in the head only (panel A), tail only (panel B), head and tail (wild type k5, panel C) or cysteine minus k5 (panel D) were treated with CE-MTS, separated from unincorporated CE-MTS and assembled with an equal molar amount of k18. The scale bar located in the bottom of each panel represents 200 nm.

Figure 7. EPR spectra from keratin 8 samples mixed with k18 161 spin.

As indicated in the individual groups of overlaid spectra, each k8 spin labeled protein was mixed with k18 161 spin and spectra recorded from individual urea concentrations. In the lower right, k18 161 was mixed with non-spin-labeled k5 as a k18 alone control.

Figure 8. EPR spectra from keratin 8 samples mixed with k18 165 spin.

As indicated in the individual groups of overlaid spectra, each k8 spin labeled protein was mixed with k18 165 spin and spectra recorded from individual urea concentrations. In the lower right, k18 165 was mixed with non-spin-labeled k5 as a k18 alone control.

Figure 9. EPR spectra from keratin 8 samples mixed with k18 168 spin.

As indicated in the individual groups of overlaid spectra, each k8 spin labeled protein was mixed with k18 168 spin and spectra recorded from individual urea concentrations. In the lower right, k18 168 was mixed with non-spin-labeled k5 as a k18 alone control.

Figure 10. EPR spectra from keratin 8 samples mixed with k18 171 spin.

As indicated in the individual groups of overlaid spectra, each k8 spin labeled protein was mixed with k18 171 spin and spectra recorded from individual urea concentrations. In the lower right, k18 171 was mixed with non-spin-labeled k5 as a k18 alone control.

Figure 11. EPR spectra from keratin 18 samples mixed with k8 351 spin.

As shown in each group of overlaid spectra, spin labeled k18 proteins were mixed with k8 spin labeled at position 351 and spectra recorded at various urea concentrations.

Figure 12. EPR spectra from keratin 18 samples mixed with k8 353 spin.

As shown in each group of overlaid spectra, spin labeled k18 proteins were mixed with k8 spin labeled at position 353 and spectra recorded at various urea concentrations.

Figure 13. EPR spectra from keratin 18 samples mixed with k8 357 spin.

As shown in each group of overlaid spectra, spin labeled k18 proteins were mixed with k8 spin labeled at position 357 and spectra recorded at various urea concentrations.

Figure 14. Assembly of LNDC k18.

Panel A, kIFs assembled from wild type k8/18. Panel B kIFs assembled from wild type k8 and k18 LNDC. Panel C, k8 LNDC mixed with wildtype k18. Panel D, the "double" substitution, k8 LNDC and K18 LNDC.

Figure 15. EPR spectra of k8 326 mixed with wt k18 or k18 LNDC

Spin labeled cys^{326} k8 was mixed with either wild type k18 (bottom) or k18 carrying the EBS like mutation LNDC (top). Samples were incubated in the indicated urea concentrations and spectra recorded.

Figure 16. Figure 16. EPR spectra from spin labeled k18 mixed with k8 LNDC.

Spin labeled cys^{294} k18 was mixed with either wild type k8 (bottom) or k8 carrying the EBS like mutation LNDC (top). Samples were incubated in the indicated urea concentrations and spectra recorded.

Figure 17. EPR spectra of k8/k18 mixtures treated with CEES or MEC for $_{A11}$ structure.

The assembly of keratin subunits into tetramer $_{A11}$ was analyzed using k8 spin labeled at position 196 and k18 spin labeled at position 168. Interaction between these positions is indicative of the $_{A11}$ structure. As indicated by the groupings, spin labeled proteins were either unmodified (control), or modified by CEES or MEC followed by incubation in the indicated urea concentrations and spectra were collected.

Figure 18. EPR spectra of k8/k18 mixtures treated with CEES or MEC for A_{22} structure.

The assembly of keratin proteins into the A22 tetramer was analyzed using k8 spin labeled at position 357 and k18 spin labeled at position 323. Interaction between these positions is indicative of the A22 structure. Three sets of reactions were analyzed: unmodified keratins, CEES modified, or MEC modified. Spectra from these reactions were recorded from appropriate mixtures in the indicated urea concentrations.

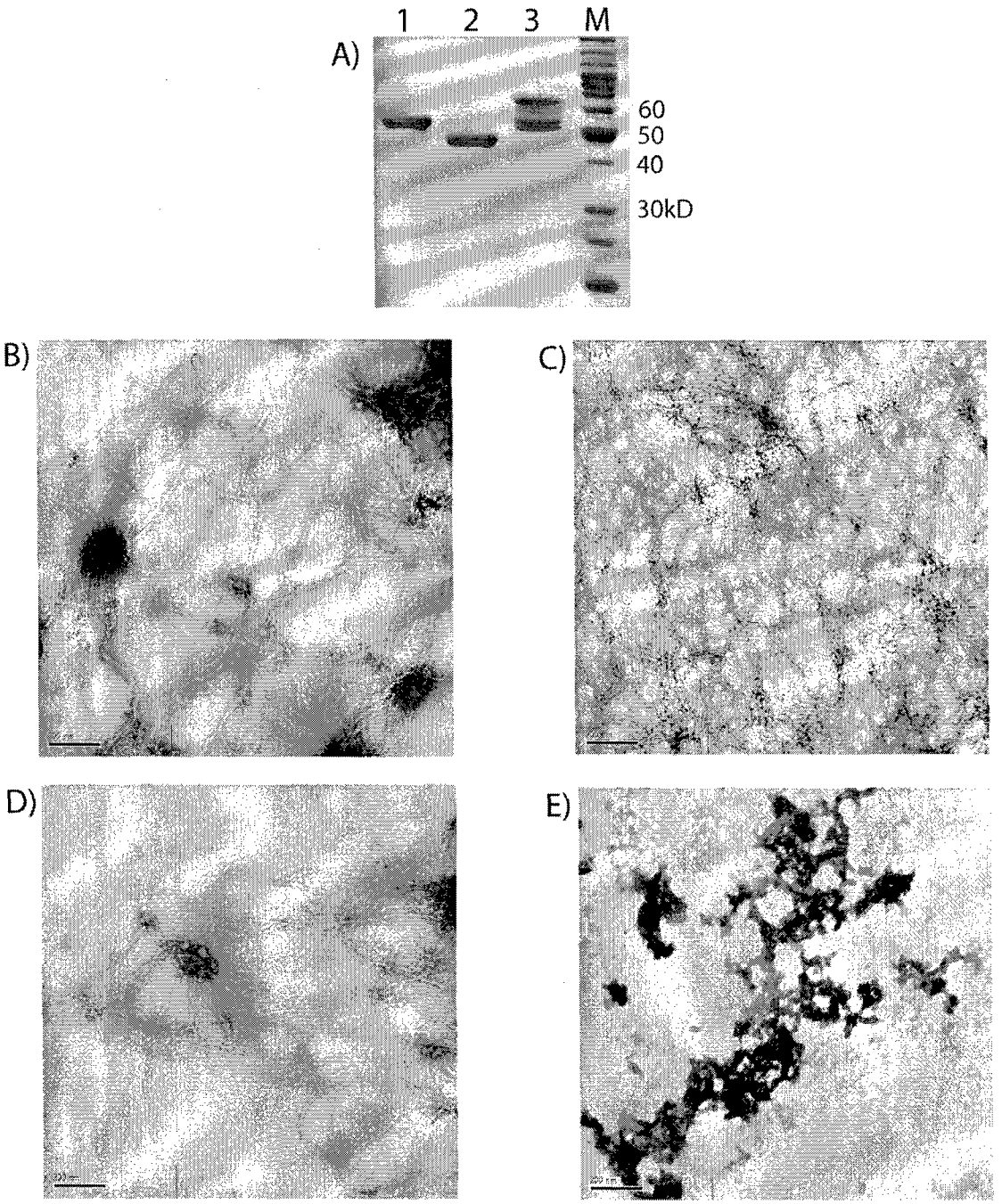

Figure 1. Keratin protein isolation and assembly

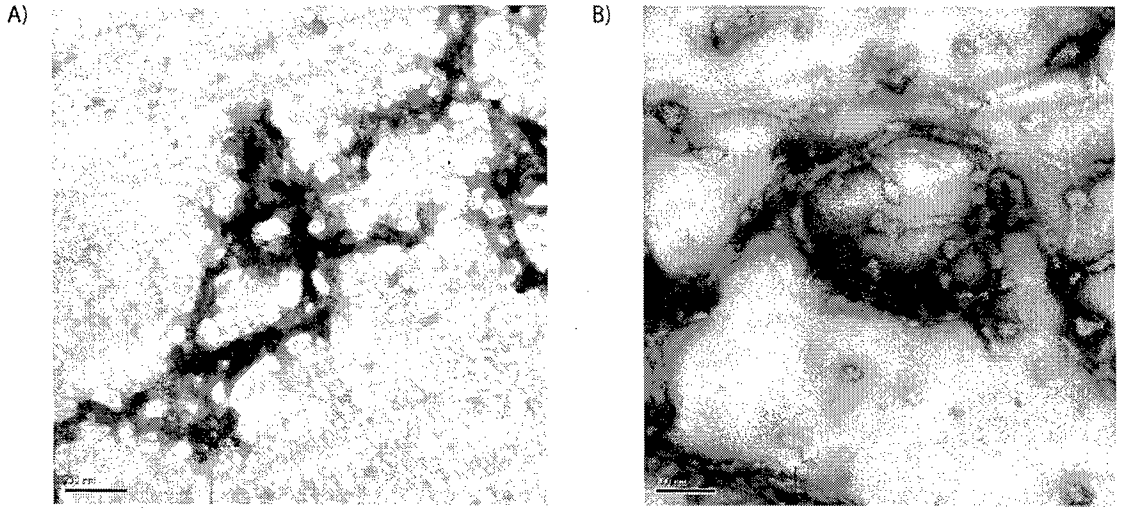

Figure 2. Treatment of intact kIFs with CEES or MEC.

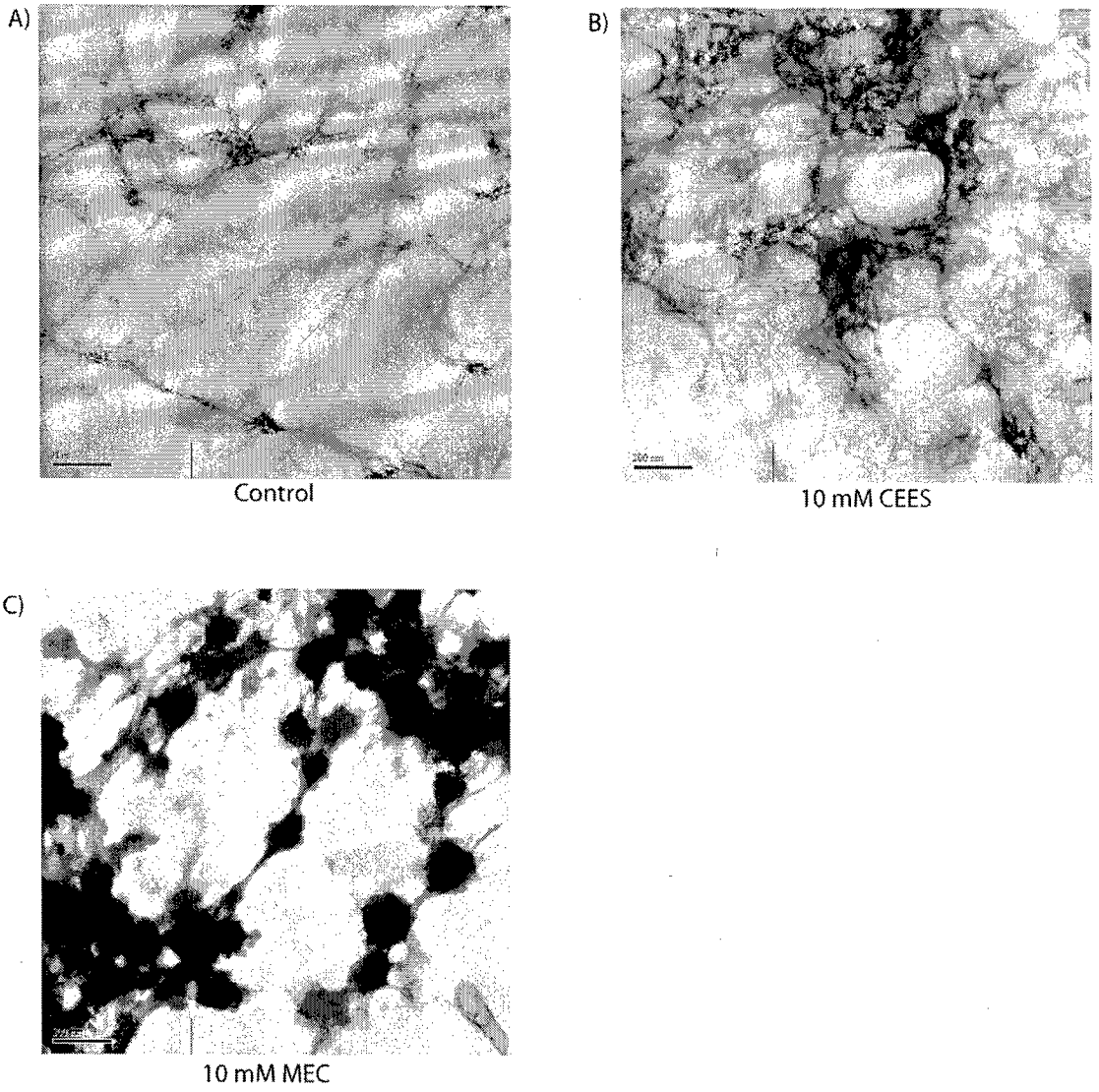

Figure 3. Treatment of keratin monomers with SM analogs followed by assembly.

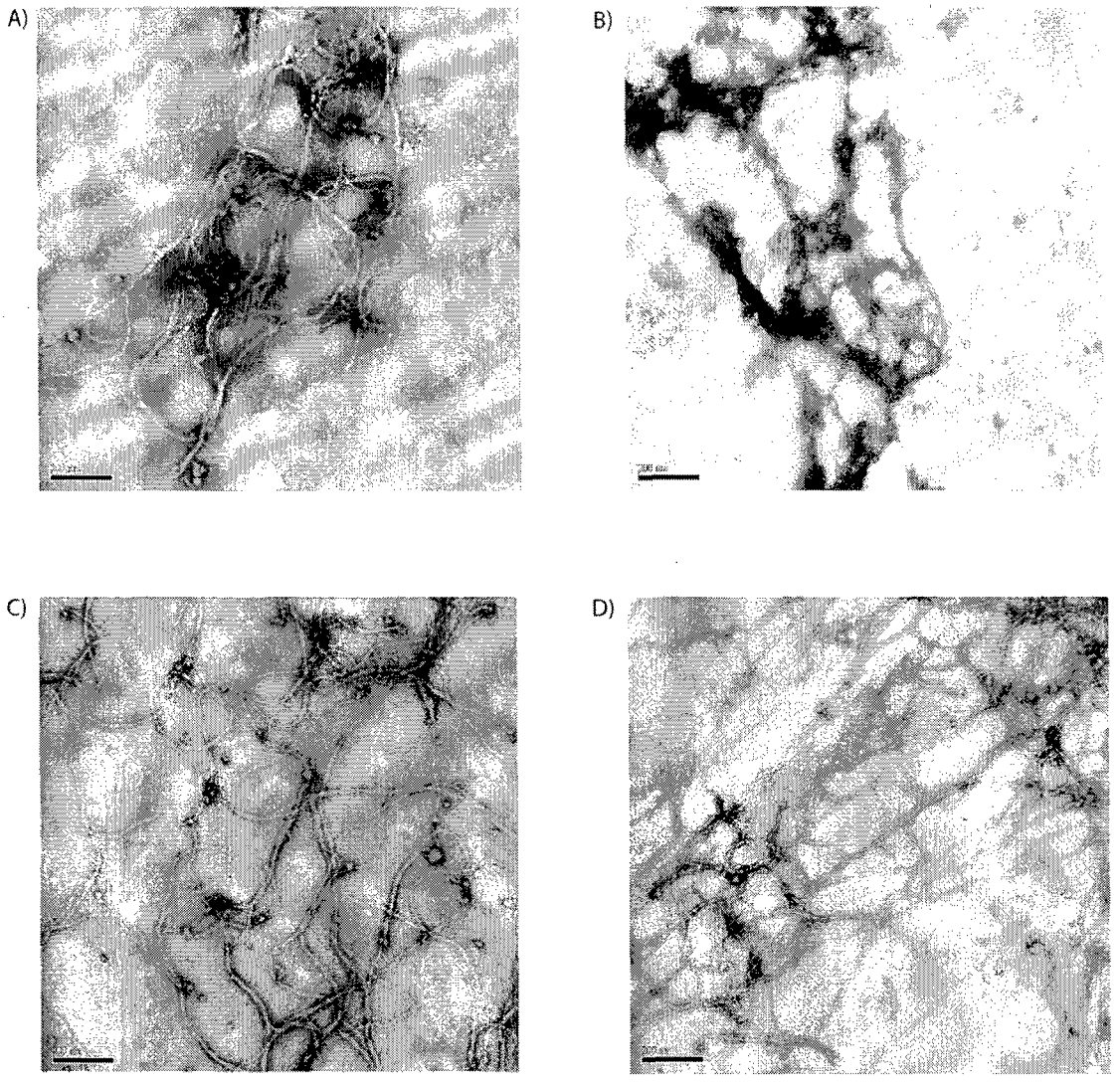

Figure 4. Sulfhydryl modification of bovine keratins

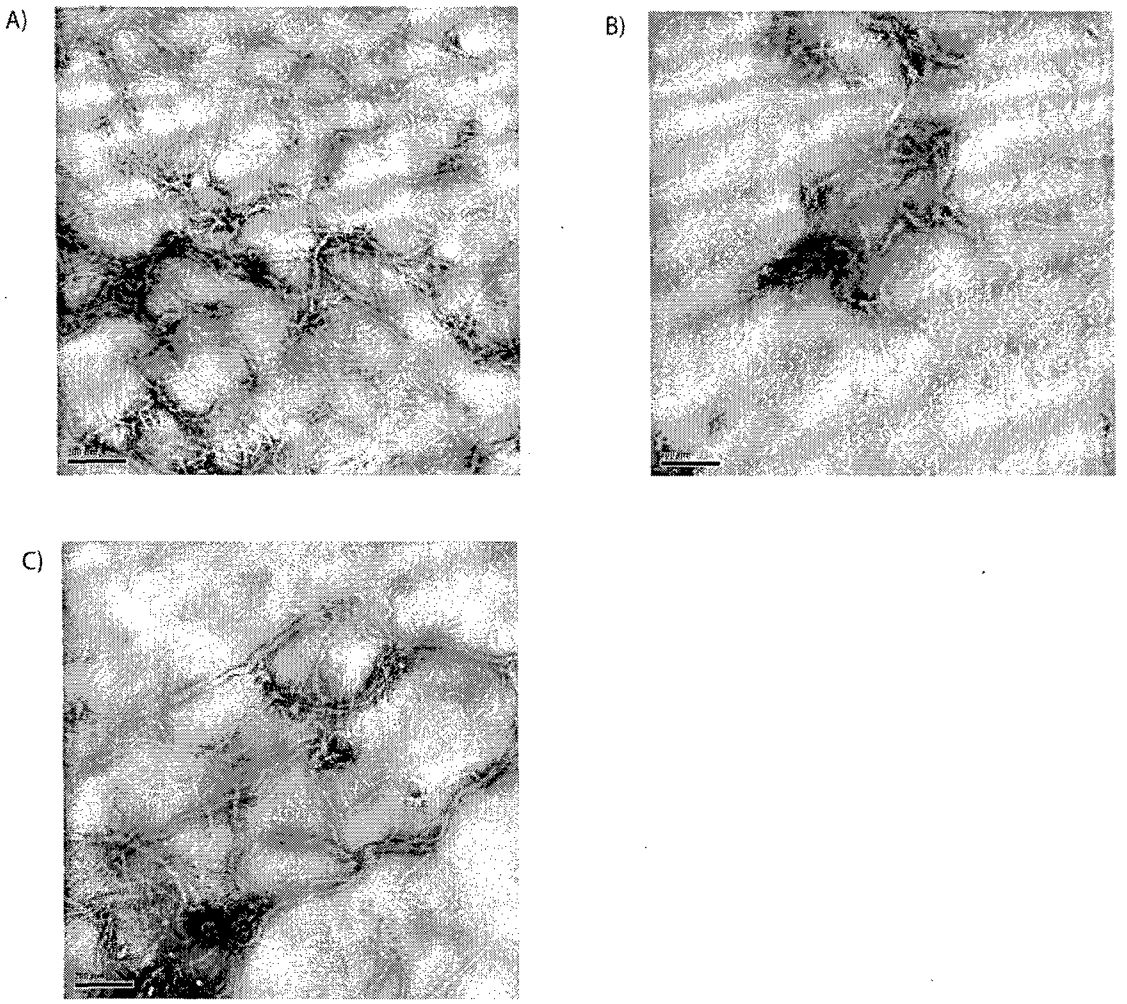

Figure 5. Mixing of modified keratins with unmodified keratins.

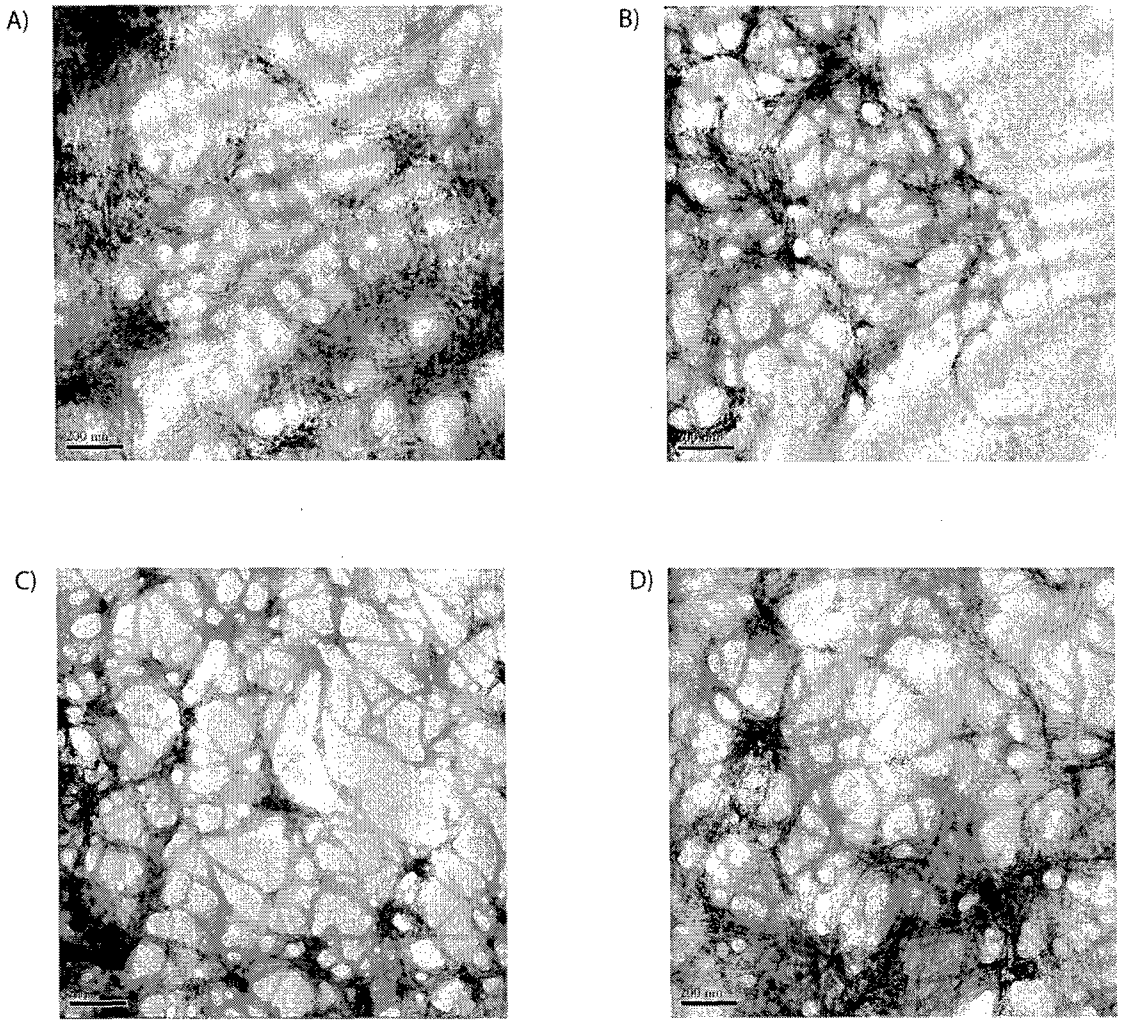

Figure 6. CE-MTS modification of K5 mutants.

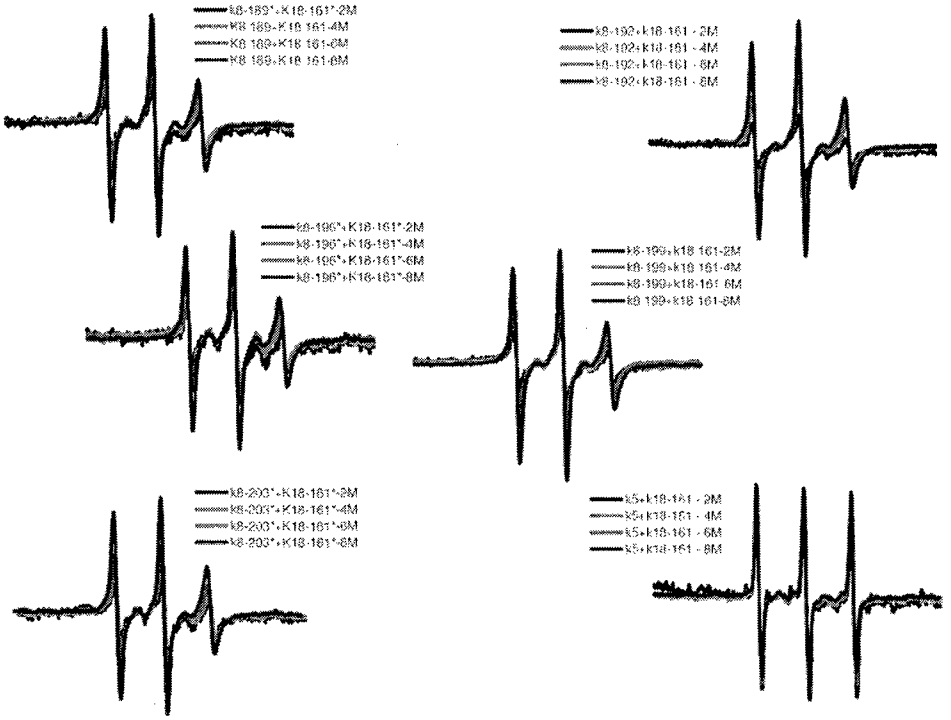

Figure 7. EPR spectra from mixtures including k18 161spin.

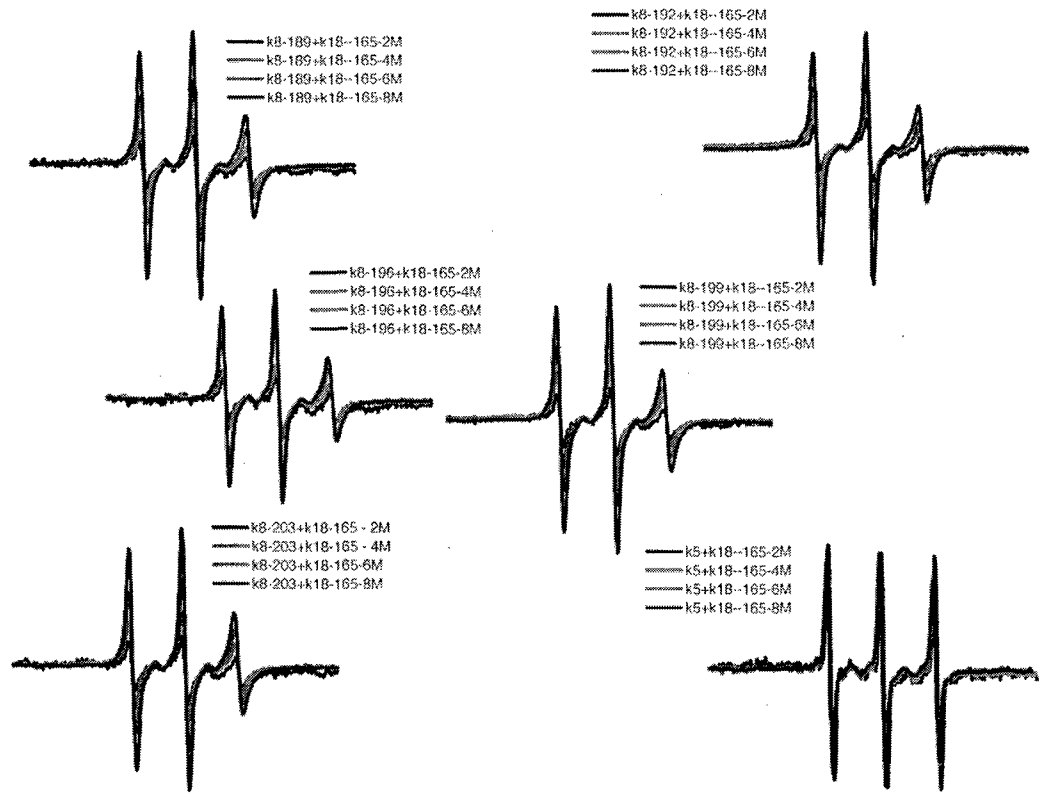

Figure 8. EPR spectra from mixtures including k18 165 spin.

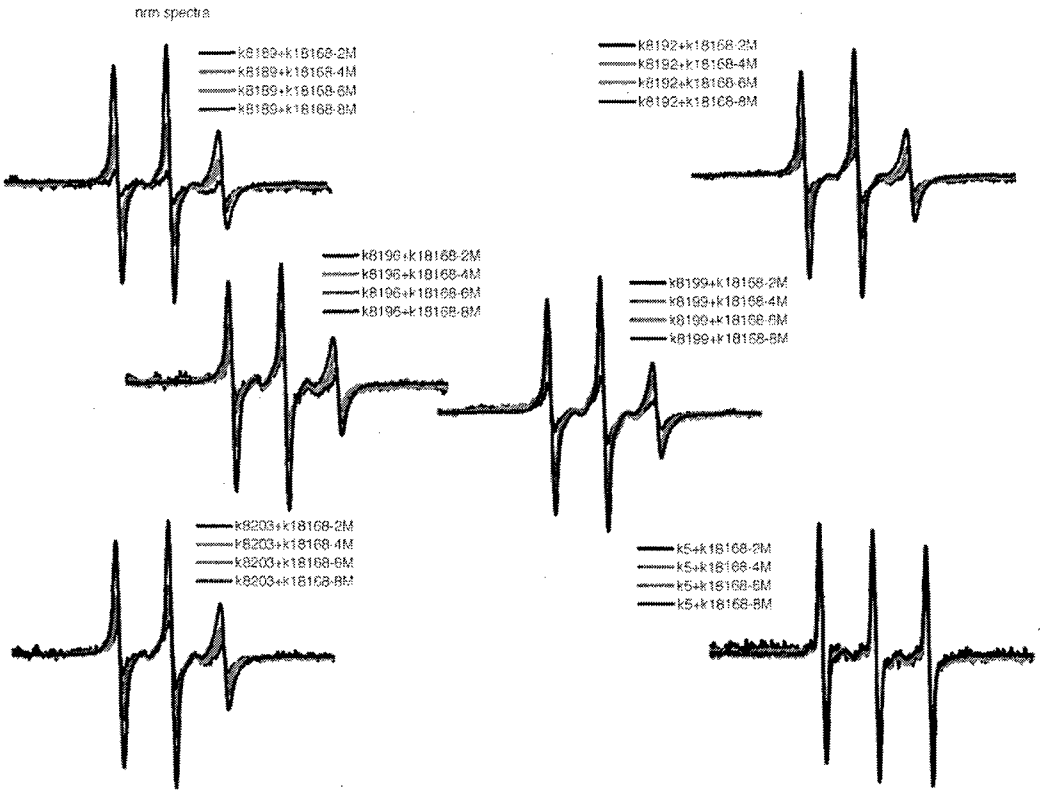

Figure 9. EPR spectra from mixtures including k18 168 spin.

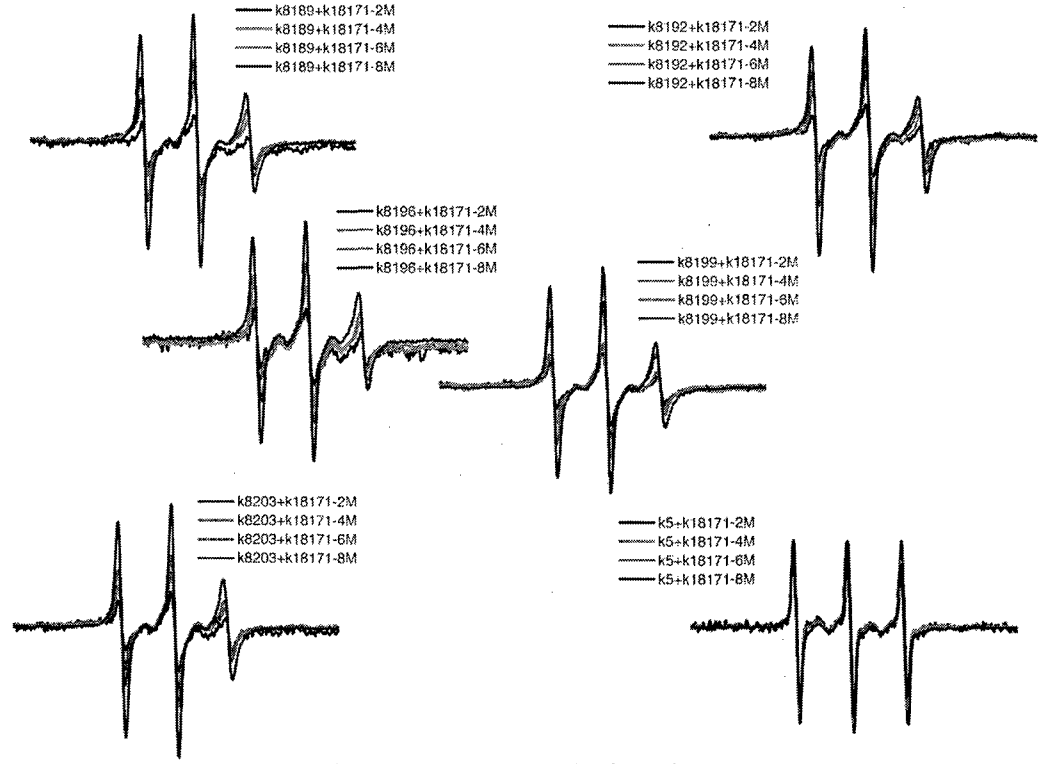

Figure 10. EPR spectra from mixtures including k18 171 spin.

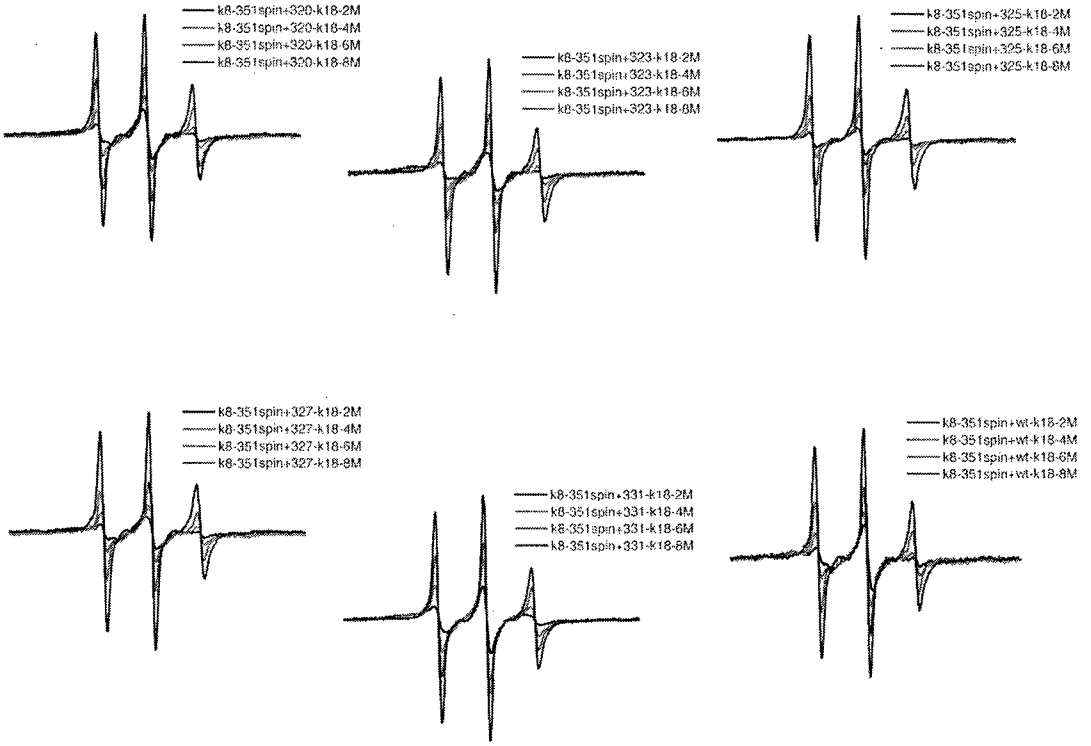

Figure 11. EPR spectra from keratin mixtures including k8 351 spin.

Figure 12. EPR spectra from keratin mixtures including k8 353 spin.

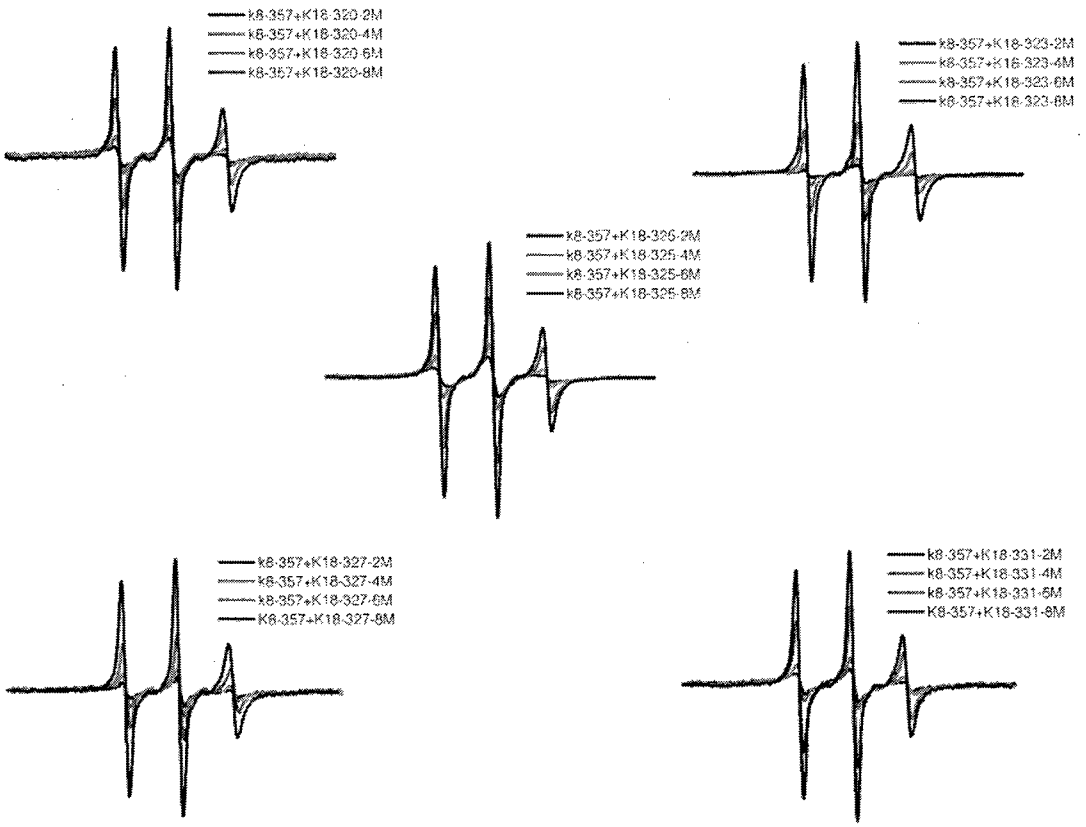

Figure 13. EPR spectra from keratin mixtures including k8 357 spin.

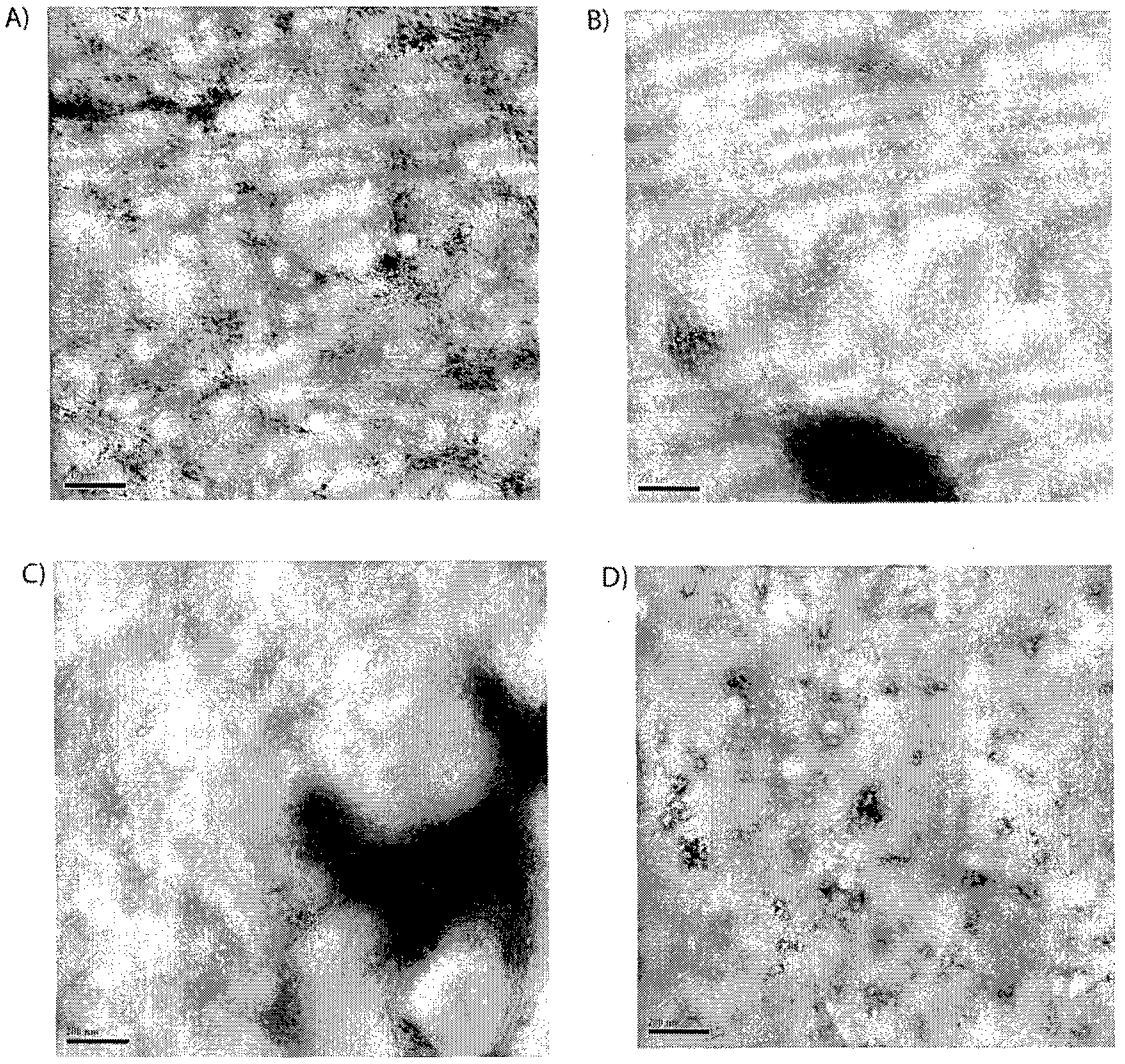

Figure 14. Keratin LNDC mutant assembly.

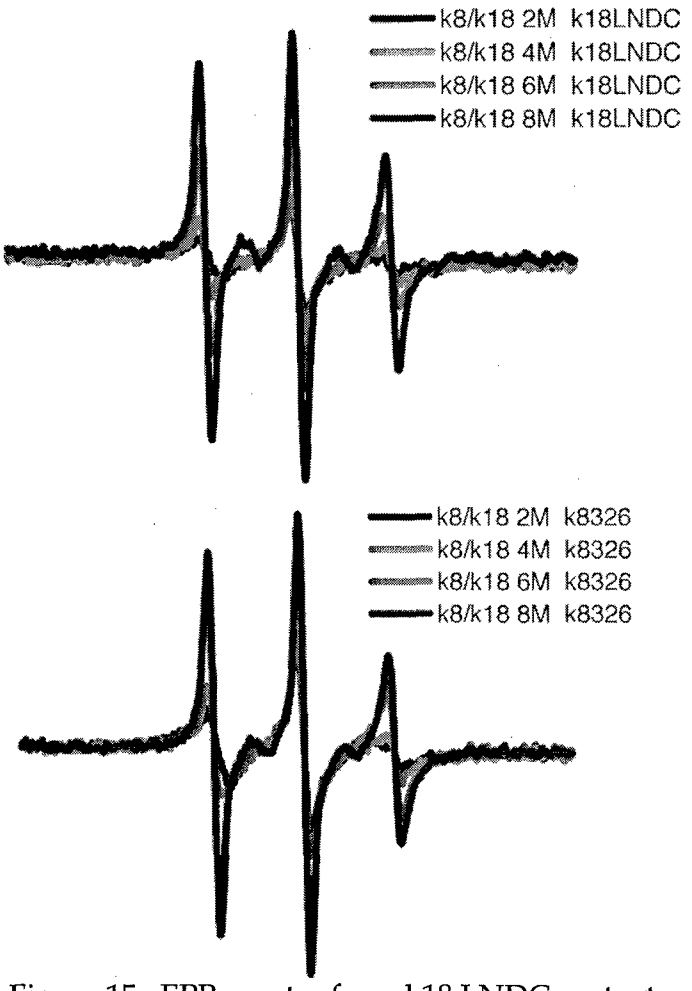

Figure 15. EPR spectra from k18 LNDC mutants.

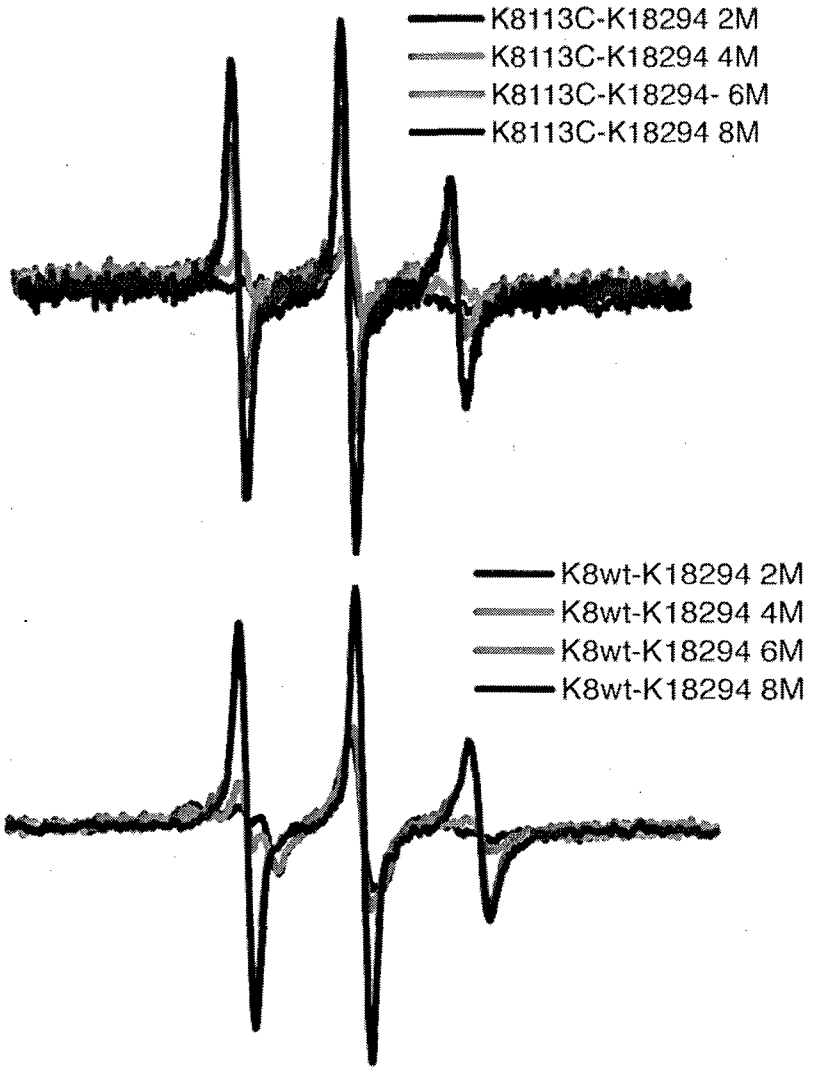

Figure 16. EPR spectra from spin labeled k18 mixed with k8 LNDC.

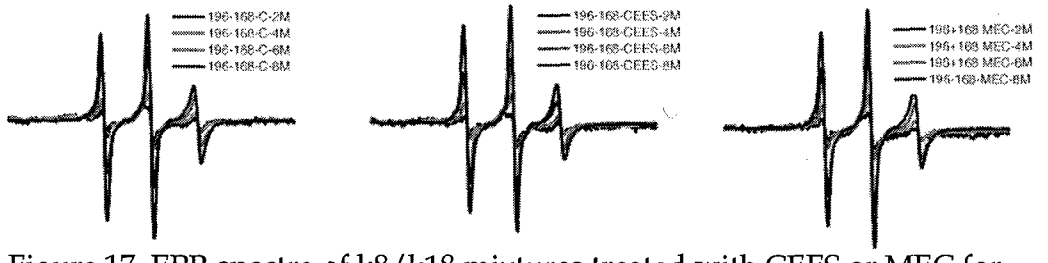

Figure 17. EPR spectra of k8/k18 mixtures treated with CEES or MEC for $_{A11}$ structure.

Figure 18. EPR spectra of k8/k18 mixtures treated with CEES or MEC for the A_{22} structure.

THE JOURNAL OF BIOLOGICAL CHEMISTRY
Vol. 280, No. 3, Issue of January 21, pp. 2141–2146, 2005
Printed in U.S.A.

Characterization of Structural Changes in Vimentin Bearing an Epidermolysis Bullosa Simplex-like Mutation Using Site-directed Spin Labeling and Electron Paramagnetic Resonance*

Received for publication, October 28, 2004
Published, JBC Papers in Press, November 18, 2004, DOI 10.1074/jbc.M412254200

John F. Hess‡, Madhu S. Budamagunta§, Paul G. FitzGerald‡¶, and John C. Voss§

From the ‡Department of Cell Biology and Human Anatomy, §Department of Biological Chemistry. School of Medicine, University of California, Davis, California 95616

Mutations in intermediate filament protein genes are responsible for a number of inherited genetic diseases including skin blistering diseases, corneal opacities, and neurological degenerations. Mutation of the arginine (Arg) residue of the highly conserved LNDR motif has been shown to be causative in inherited disorders in at least four different intermediate filament (IF) proteins found in skin, cornea, and the central nervous system. Thus this residue appears to be broadly important to IF assembly and/or function. While the genetic basis for these diseases has been clearly defined, the inability to determine crystal structure for IFs has precluded a determination of how these mutations affect assembly/structure/function of IFs. To investigate the impact of mutation at this site in IFs, we have mutated the LNDR to LNDS in vimentin, a Type III intermediate filament protein, and have examined the impact of this change on assembly using electron paramagnetic resonance. Compared with wild type vimentin, the mutant shows normal formation of the coiled coil dimer, with a slight reduction in the stability of the dimer in rod domain 1. Probing the dimer-dimer interactions shows the formation of normal dimer centered on residue 191 but a failure of dimerization at residue 348 in rod domain 2. These data point toward a specific stage of assembly at which a common disease-causing mutation in IF proteins interrupts assembly.

The intermediate filament (IF)[1] protein gene family consists of about 60 members at present. While primary sequence among the family members shows a considerable degree of sequence variation, the vast majority of IF proteins show conservation of a predicted domain structure. This structure consists of a central rod domain whose predicted secondary structure is well conserved, and head and tail domains, where both size and primary sequence, are more variable. While the predicted secondary structure of the central rod domain is conserved, there is much primary sequence variability except at two small motifs located at either end of the central rod domain. At these sites, sequence conservation has been quite strong. These two motifs have been referred to as the "rod initiation" and "rod termination" motifs. Not surprisingly, a disproportionate fraction of human disease-causing mutations in IF proteins are found in these highly conserved motifs (1–11).

In the early 1990s, three lines of evidence independently identified IF protein genes as the site of mutations leading to epidermolysis bullosa simplex (EBS) and other skin blistering diseases in humans such as epidermolysis hyperkeratosis (3, 5, 12–19). First, Fuchs and co-workers (20) working in cell culture and mouse systems showed that cytokeratin mutations gave rise to EBS-like defects in mice. Second, genetic linkage analysis in humans indicated that keratin genes were involved in skin blistering diseases (1). Third, keratin mutants were identified on the basis of abnormal antibody binding, caused by changes in the primary sequence of epidermal IF protein (13). Subsequent characterization of additional EBS cases revealed a hotspot for mutations at the conserved motif LNDR, located at the beginning of the central rod domain. Commonly, a point mutation in the IF gene led to an Arg → His (12) or Arg → Cys mutation in this motif (12, 21). Subsequently, mutations in the cornea-specific keratins K3 and K12 at the same LNDR sequence were shown to segregate with a corneal dystrophy phenotype (22–24). Most recently, the same region in GFAP has been shown to be the site of mutations leading to the neurodegenerative Alexander disease (25). Thus, the fourth residue of this LNDR motif appears to be of critical importance to several IF proteins, from multiple classes of IF.

The mechanism of these genetic mutations seems clear. Alteration of the arginine codon (CGN) is consistent with the hypothesis that CpG dinucleotides are sites of methylation-induced deamidation of cytosine, leading to a Cys → Thr transition (CGY → TGY cysteine codon) (26). However, the structural impact of this Arg → Cys substitution on IF assembly and structure remains poorly defined, as IF proteins and IFs have not been crystallized. Whether the result of *in vitro* mutagenesis or random chance, mutations in keratin genes typically have been studied *in vitro* by 1) analysis of the assembly characteristics of the mutant proteins and 2) the ability of the mutant proteins to assemble into intermediate filament networks in transfected cells. In general, there is a good correlation between the severity of skin blistering seen in a clinically affected individual and the magnitude of assembly abnormalities seen when the mutant protein is analyzed *in vitro* (19). Thus, mutants that fail to form filaments *in vitro* and fail to integrate into cellular IF networks in cell culture produce the worst cases of skin blistering. Analysis of the effect of specific mutations on keratin assembly has been described by Steinert and co-workers (27, 28) who designed an experimental protocol

* This work was supported by Grant DAMD017-02-1-0664 (to J. H.) from the United States Army Medical Research and Material Command, National Institutes of Health Grant RO1 NEI EY08747 (to P. G. F.), and March of Dimes Grant 5-FY02-202 (to J. C. V.). The costs of publication of this article were defrayed in part by the payment of page charges. This article must therefore be hereby marked "*advertisement*" in accordance with 18 U.S.C. Section 1734 solely to indicate this fact.

¶ To whom correspondence should be addressed. Tel.: 530-752-7130; Fax: 530-752-8520; E-mail: pgfitzgerald@ucdavis.edu.

[1] The abbreviations used are: IF, intermediate filament; EBS, epidermolysis bullosa simplex; SDSL-EPR, site-directed spin labeling electron paramagnetic resonance.

based on the cross linking between proteins at different urea concentrations. Cross-linking between proteins reflects the proximity of the cross linking moieties and thus can be used to establish whether normal interactions have/have not occurred during assembly. Specifically, comparison of cross-links in mutant proteins to those formed in wild type proteins can be used to infer whether distances between cross-linking moieties have changed as a result of the mutation. Since IF proteins will undergo stepwise assembly when dialyzed out of high concentrations of urea or guanidine, these cross-linking studies can be performed on intermediates of assembly, providing data relevant to the stage of assembly affected by the mutation (29).

Mehrani *et al.* (27) showed specifically that K14 LNDR mutated to LNDL was unable to form IFs, unable to assemble into existing IF networks in cells, and was significantly altered in the tetramer configuration. Lys^{14} LNAR was similarly unable to form filaments *in vitro* and unable to integrate into IF networks but exhibited slightly less stability than the wild type. They summarize the characterization of these substitutions in the Asp and Arg locations of LNDR as significantly destabilizing the two-molecule entities (tetramer).

Following the demonstration of the applicability of site-directed spin labeling electron paramagnetic resonance (SDSL EPR) to the study IF structure (30, 31), we began a series of experiments designed to test the hypothesis that EPR can be used to identify the effects of mutations on IF assembly. To perform these experiments, EBS-like mutations (LNDR → LNDS and NDR → LNDC) were engineered into human vimentin (1). *In vitro* assembly verifies that assembly is aborted very early in the process with both mutants failing to assemble into 10-nm filaments. Because the spin labeling protocol that we employ targets cysteine residues, we have used a vimentin LNDR → LNDS mutant to study the impact of mutations at this site on assembly. In previous work we have identified specific "reporter" residues within vimentin that, when spin-labeled, reveal whether specific stages of assembly have occurred and when in the course of assembly they occur. We can therefore discriminate between mutations that affect initial coiled coil dimer formation, or subsequent dimer-dimer interactions. Using this approach we report the impact of EBS-like mutations on the assembly of the Type III IF protein vimentin.

MATERIALS AND METHODS

Vimentin characterization, mutation, cloning, expression, purification, and spin labeling were described in detail in a previous reports (30, 31). In brief, the spin label is ultimately attached to cysteine residues that are targeted to specific sites in vimentin. Cysteine codons were introduced into the vimentin expression construct (generously provided by Dr. Roy Quinlan, University of Durham, Durham, UK) using the Stratagene QuikChange kit (Stratagene, La Jolla, CA). Combinations of mutations (for example, Ser^{113} plus Cys^{191}) were created, where possible, by cloning of restriction fragments, each containing one mutation, together into an expression vector. If not possible, then mutagenesis was performed in a sequential fashion. Sequence changes were verified by DNA sequencing. Mutant vimentin was produced by bacterial expression and purified from inclusion bodies using high/low salt washes, and chromatography. Spin labeling was accomplished by incubation of the purified vimentin in 100 μM tris-(2-carboxyethyl)phosphine (Molecular Probes, Eugene, OR) followed by 500 μM O-87500 (Toronto Research Chemicals, Toronto, Canada). Unincorporated spin label was removed by CM-Sepharose chromatography using a GE Healthcare FPLC (30, 31). Labeled proteins were stored long term at −80 °C.

Filament assembly was performed either as a single step dialysis against filament assembly buffer or as a stepwise process following the protocol of Carter *et al.* (32) Briefly, labeled proteins were solubilized in 8 M urea, which was then removed by dialysis, either in a single step procedure, or where indicated, in a stepwise process through progressively reduced concentrations of urea, followed by low ionic strength Tris, followed by the addition of NaCl and $MgCl_2$. Filament assembly was verified by electron microscopy of negatively stained samples.

EPR was conducted on a JEOL X-band spectrometer equipped with a loop gap resonator. Approximately 4 μl of sample, at a concentration of 25–75 μM protein, were placed in a sealed quartz capillary tube. Spectra were acquired at 20–22 °C with a single 60-s scan over 100 G at a microwave power of 2 milliwatts and a modulation amplitude optimized to the natural line width of the attached nitroxide.

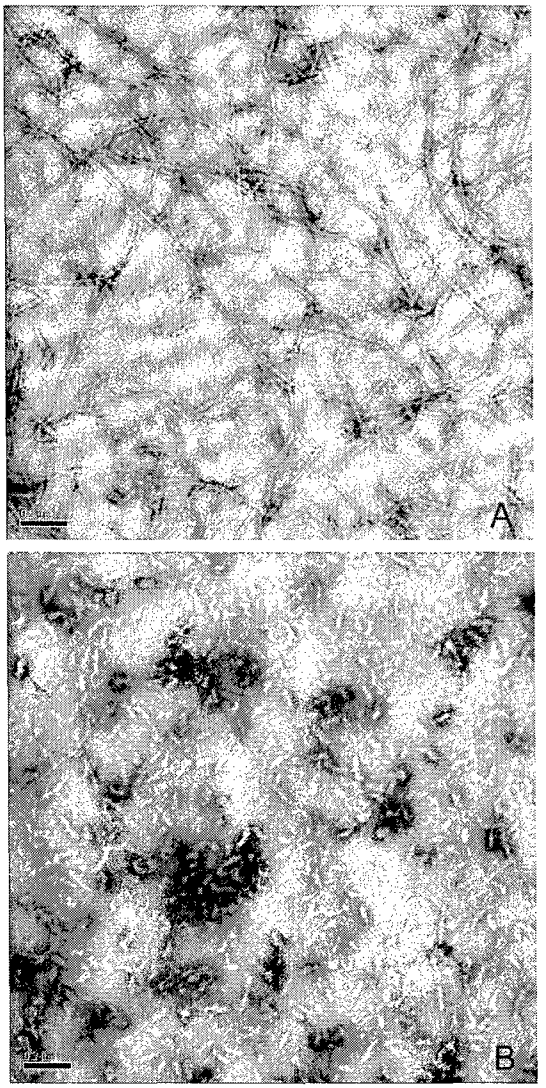

FIG. 1. **Electron microscopy of wild type and mutant vimentin assembled *in vitro*.** *A*, control showing a negatively stained preparation of cysteine-free vimentin, used as a starting point for subsequent studies. Long, uniformly shaped 10-nm filaments are evident. *B*, negatively stained preparation of vimentin bearing the LNDS mutation. Filament assembly is blocked at a very early stage, resulting in a population of small, uniformly sized particles.

RESULTS

Electron microscopy cysteine-free vimentin (Cys^{328} → Ser) used as a starting point for subsequent studies shows long uniform filaments, which are morphologically indistinguishable from wild type vimentin (Fig. 1*A*). In contrast, vimentin bearing the LNDR → LNDS mutation failed to form recognizable filaments (Fig. 1*B*). In these preparations, assembly was aborted at a very early stage, yielding uniformly small "rodlets." Vimentin bearing the LNDC mutation similarly caused a very early failure in the assembly process, yielding aggregates of small particles (not shown).

We then used site-directed spin labeling followed by EPR spectroscopy to examine the structural and assembly consequences of the R113S (LNDR to LNDS) mutation (Fig. 2). We have previously shown that SDSL EPR yields structural infor-

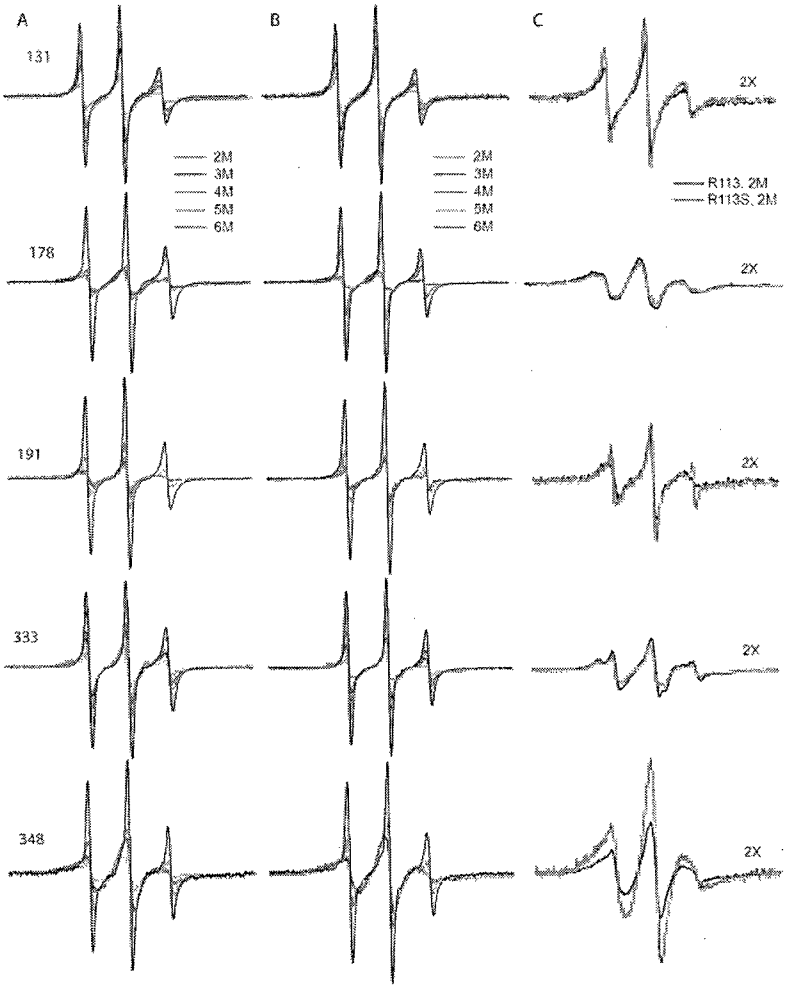

FIG. 2. **EPR spectra of spin-labeled vimentin at selected positions.** The residue location of the spin label is indicated for each row of spectra. *A*, spectra from the indicated position when vimentin contains the native residue at position 113 (Arg^{113}). *B*, spectra of the spin-labeled residues in combination with the LNDR mutation $Arg^{113} \rightarrow$ Ser. In *A* and *B*, each spectrum represents the signal in the presence of 2–6 M urea (see key for colored lines), and all spectra are normalized to an identical concentration of spin-labeled protein. *C*, comparison of the EPR spectra at 2 M urea when protein contains either native Arg^{113} (*black trace*) or the LNDR mutation $Arg^{113} \rightarrow$ Ser (*red trace*). To facilitate a comparison, the spectra in *C* are magnified by a factor of 2 over the spectra in *A* and *B*.

mation at several levels in intact IFs, as well as in assembly intermediates that form during *in vitro* assembly. Depending on the specific site that is labeled, EPR can monitor the assumption of α helical structure, the formation of coiled coil dimers, and the formation of subsequent higher order interactions between dimers, either in intact filaments or at specific stages during *in vitro* assembly that occur as filament protein is dialyzed out of 8 M urea. We approached this by creating the R113S mutation and then placing spin labels at different locations within the mutant protein to monitor the impact that this mutation produced at the spin labeled site (a schematic indicating the relative locations of these mutants is presented in Fig. 3).

To examine the impact of the R113S mutation on α helical, coiled coil dimer formation, we first evaluated the spectral changes as a function of urea concentration of protein containing the wild type Arg^{113}, with the spin label located at either position 178 (a *d* position in rod domain 1) or 333 (a *d* position in rod domain 2). Spin labels at these sites provide data about 1) secondary structure (α helix formation) and 2) coiled coil formation, since these two residues would be within 2 nm of each other in a coiled coil dimer. As demonstrated previously (30, 31), *a,d* positions within a coiled coil generate a characteristic immobilized and dipolar-broadened spectrum when the urea concentration is lowered to 2 M. In the wild type vimentin, a tightly packed environment at position 178 (rod 1) occurs earlier and is almost completely achieved at 4 M urea, whereas a strongly broadened spectrum from position 333 (rod 2) is not achieved until 2 M urea (Fig. 2*a*). The magnified spectra for spin labeled 178 and 333 at 2 M urea are shown in Fig. 2*c*. This observation suggests that in wild type vimentin, coiled coil formation occurs more readily in rod domain 1B in the region surrounding position 178 than in rod domain 2 near position 333.

We then repeated these studies but now using vimentin bearing the R113S mutation. In the presence of the R113S mutation, position 178 remains flexible at 4 M urea (Fig. 2*b*), indicating the LNDS mutation causes a slight perturbation in coiled coil formation in rod 1B. In contrast, the increased broadening at position 333 in rod 2 occurs just as readily in the LNDS mutant as it does in vimentin that contains the wild type Arg^{113} (Fig. 2*b*). This suggests that the presence of the mutation at residue 113 (rod domain 1) has little impact on the formation of the coiled coil dimer in rod domain 2 but does affect the ability of rod domain 1 to undergo normal α helical coiled coil assembly.

To further investigate the impact of this mutation on early assembly, we placed a spin label closer to the LNDR motif at position 131. Position 131 is predicted to be a (*d*) position at the end of rod 1A. As shown in Fig. 2*A*, vimentin with a label located at 131 does not display the characteristic broad spectrum of an *a/d* position (see "Discussion"). A slight effect of the LNDS mutation is observed at position 131. As shown in Fig. 2*C*, the spectrum of spin-labeled 131 in 2 M urea is somewhat sharper, suggesting that the R113S mutation may impart further destabilization to this region of the protein.

We have shown in previous work that residues 191 (rod 1) and 348 (rod), both of which are non *a,d*, positions and therefore on the outside of the coiled coil dimer (see Fig. 3), can be used to monitor the formation of interactions between vimentin dimers during filament assembly studies (30, 31). These stud-

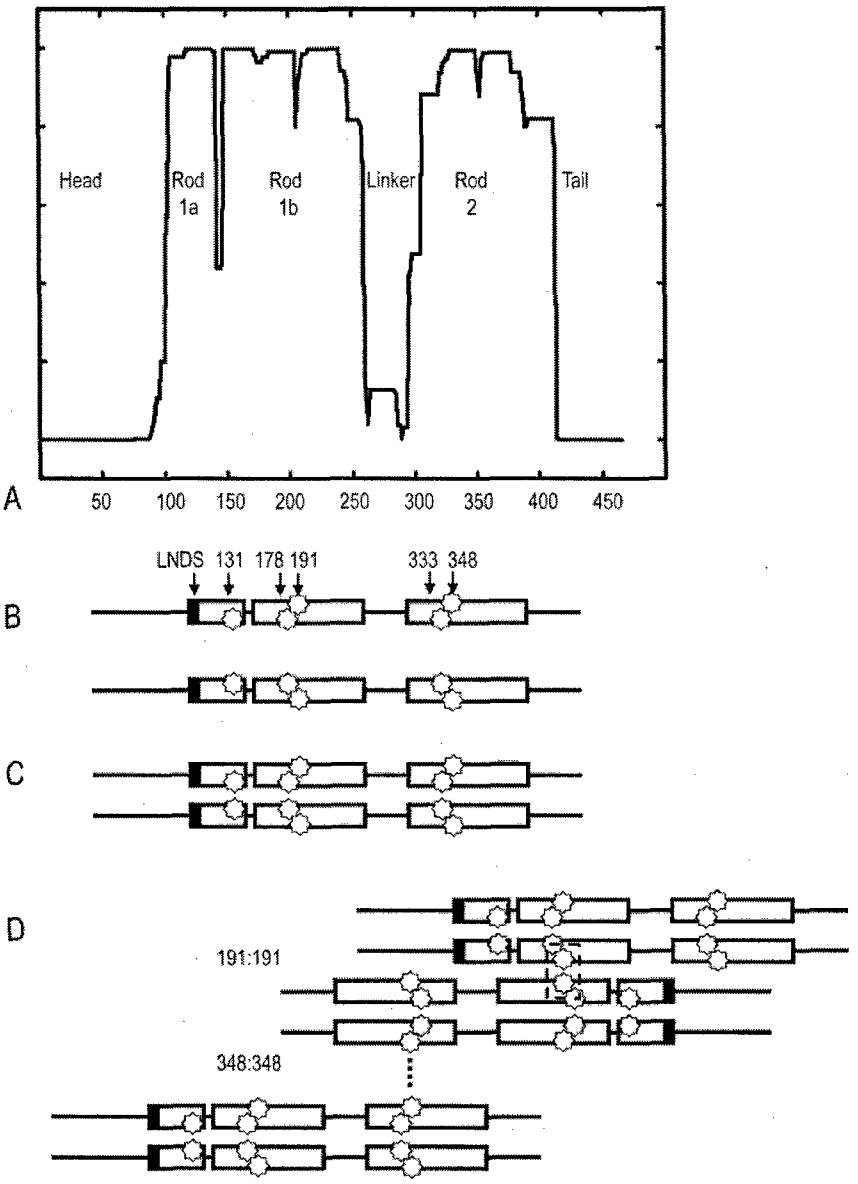

FIG. 3. **Schematic of vimentin predicted domain structure and spin label placement.** *A*, coils prediction (44) of human vimentin. The boundaries of the central rod domain, as well as the linker regions, are based on predictions of coiled coil structure and yield a domain structure depicted in *A*. *B*, schematic of a vimentin monomer, with LNDS motif, and the specific spin label reporter residues indicated at their approximate locations. Note that residues 131, 178, and 333 are *a,d* positions in the heptad and are located at the interface between two monomers. Residues 191 and 348 are non *a,d* positions and are located on the exterior surface of a dimer. *C*, schematic indicating dimer formation. *D*, schematic indicating that in the LNDS mutant, the 191:191 dimer forms, while the 348:348 dimer does not, as assessed by EPR using these residues as reporters for activity at these sites.

ies established that dimers interact at residue 191 (rod domain 1) before interactions occur at residue 348 (rod domain 2) thus establishing a sequence of dimer-dimer interactions during *in vitro* assembly. To evaluate the impact of the R113S mutation on these interactions, we spin-labeled proteins individually at both 191 and 348. Examination of mutant protein labeled at residue 348 (an *e* position in rod 2) shows that, in the range of 6–3 M urea, the R113S mutant behaves similarly to the wild type protein (Fig. 2, *A versus B*). This is consistent with the data derived from mutants labeled at residue 333, indicating normal secondary structure in rod domain 2. However, as described below, the R113S mutation produces a loss of the dipolar broadening of spin label placed at residue 348 that arises at 2 M urea in wild type protein. This suggests that the approximation of two dimers centered around residue 348 fails to occur in a normal manner.

While the LNDS mutation causes a small fraction of the spin labels at 191 to remain highly mobile at low urea levels, the level of dipolar broadening compared with protein with native Arg^{113} is unchanged, indicating that a magnetic interaction occurs between labels located at 191, as R113S vimentin dimers assemble into higher ordered structures. Thus the A_{11} alignment, as measured by dipolar interaction at 191, is not detectably perturbed by the R113S mutation. In contrast, evidence for A_{22} alignment, as reported by labels placed at position 348, is completely eliminated in vimentin containing the R113S mutation. This difference is highlighted in Fig. 2*C*, where the normalized 2 M urea spectra of spin-labeled 348 with and without the LNDS mutations are compared. From this we conclude that the R113S mutation permits the formation of coiled coil dimers in rod 2 but that the mutation has a demonstrable impact on the dimer-dimer interactions that should occur in rod 2.

DISCUSSION

The helix initiation and termination motifs of IF proteins have proven to be "hotspots" for mutations that result in a disease phenotype. In the helix initiation motif (LNDR) a frequent cause of disease is mutation of the Arg residue, commonly to a Cys or His. Mutation of this site has proven causative for human diseases in the Type I cytokeratins (e.g. skin blistering and corneal dystrophies) but also in the Type III IF protein GFAP as well (1, 3, 5, 14, 16, 19, 21, 22, 25, 33). Thus this specific site appears to be critical to normal assembly in multiple IF proteins from more than one class, suggesting that the data derived from study of this mutation may be broadly

applicable. An interesting side note is that the lens-specific intermediate filament protein, CP49, shows striking divergence at this motif (LGGC) that includes a Cys in the fourth position (LGGC) (34, 35).

While the exact nucleic acid changes resulting in these diseases have been identified, the impact of each mutation on assembly, structure, and function of the IFs has proven far more difficult to define. This difficulty largely derives from the inability to develop crystals of intact IF proteins or of intact IFs. While progress has been made in determining crystal structure of fragments of the IF protein vimentin (36, 37), the capacity to study structure in intact proteins, or in intact IFs, remains elusive. Thus, the means by which a specific disease-causing mutation alters or aborts assembly of IFs has remained difficult to approach experimentally. Because IFs must integrate into the biology of the cell, EBS-type mutations may result from changes that are permissive to filament assembly and/or from mutations that block the linkage between filaments and other cellular structures. Plectin, for example, links IFs to the plasma membrane. Mutations in the plectin gene that alter interactions with IFs have been identified that also result in skin blistering phenotypes (38–40). Another example is the LNDR → LNDH mutation that has also been identified as an EBS causing mutation (12). *In vitro* this mutant readily assembles into long, normal IFs, perhaps better than wild type filaments, suggesting the disease phenotype results from another mechanism and not the failure to form filaments (41).

In the absence of the crystal structure of IFs, our understanding of the structural changes caused by these many disease causing mutations is likely to result from the integration of data from several different approaches such as *in vitro* assembly, cross-linking, analytical ultracentrifugation, x-ray crystallography, and SDSL EPR.

Coulombe and co-workers (29) used cross-linking and chromatography under different denaturing conditions to characterize a proline mutant of keratin 16 and concluded that the effect of the mutant was to destabilize keratin tetramers. Steinert and co-workers (28) have developed cross-linking protocols that measure differences in the cross-linking behavior between mutant and wild type cytokeratins. These allow for the inference of how assembly and structure may be affected by these mutations (28).

Analysis of the LNDR → LNDK mutation in K14 suggested a decrease in the stability of the keratin A_{11} tetramer in urea (27). When assembled *in vitro*, this mutant forms shorter than normal filaments. Taken together, the authors conclude that decreased A_{11} tetramer stability is responsible for filament abnormalities although they leave open the possibility that these residues are important for A_{12} or A_{cn} interactions (27).

Molecular modeling of rod 1A structures and the effect of known mutations leading to EBS have suggested that LNDR → LNDS mutation in Lys^{14} produces a much greater distortion than the typical EBS mutant Lys^{14} LNDR → LNDC (42). The computer program predicts a decreased helix stability for LNDS mutation, and LNDC remains essentially unchanged. The net effect of these structural changes on higher order structures (dimers or tetramers) or filament assembly were not elucidated by the modeling. Our EM observations of vimentin show similarities between the small aggregates formed by vim Cys^{113} and vim Ser^{113}, though they were not identical.

We previously showed the ability of site directed spin labeling and electron paramagnetic resonance (SDSL EPR) to contribute to the study of IFs and IF assembly (30, 31). Using this approach we have defined specific regions of IF proteins that are involved in coiled coil dimer formation and defined the proximity of specific residues between monomers and between higher order multimers. The approach has also proven successful in defining the progression of assembly steps that occur during *in vitro* assembly, sequencing the formation of α helix, coiled coil dimer, and the sequence of specific dimer-dimer interactions.

In this report we sought to determine whether SDSL EPR could be used to define changes in IF architecture and assembly that are induced by disease-causing mutations. We elected to study the mutation of the fourth residue of the well conserved LNDR helix initiation motif, largely because mutation at this site has proven to be disease causing in several IF proteins from at least two IF classes. This suggests that this specific site is of relatively broad importance to IF assembly. We introduced the mutation in vimentin as it has been the protein from which we have gathered all initial SDSL EPR data.

In earlier work (30, 31) we showed that EPR spectra of spin labels placed at residues 178, 191, 333, and 348 display line shapes indicative of their positions within the heptad repeat, consistent with their proximity to one another in a coiled coil dimer. These residues thus serve as good indicators for the assumption/presence of coiled coil dimer at these sites. To evaluate the consequences of the LNDR → LNDS mutation we targeted spin labels to these characterized sites, as well as a site closer to the mutation in rod 1A (residue 131), and compared the spectra between wild type and R113S mutants.

The EPR spectra suggest that coiled coil dimer formation appears to proceed almost identically in the wild type and R113S mutation as monitored by spin labels at residues 178 (rod domain 1), 191 (rod domain 1), 333 (rod domain 2), and 348 (rod domain 2). A subtle difference in the EPR spectra of spin labels placed at residues 178 suggests that the transition to fully ordered structure is slightly delayed in the mutant protein, occurring somewhat later in the dialysis process than seen for the wild type. This slower attainment normal structure may be the result of decreased stability of the coiled coil dimer in this region of the mutant protein. However, upon completion of dialysis, the spectra for both mutant and wild type proteins were indistinguishable from one another, despite dramatic differences in the outcome of filament assembly between wild type and mutant proteins.

In previous work we identified several residues that serve as reporters of interactions between a given vimentin dimer and its nearest neighbors in intact filaments. Residues 191 and 348, for example, are sites of anti-parallel overlap between one vimentin dimer and other adjacent dimers in intact filaments (30, 31). We therefore compared the EPR spectra of wild type and R113S mutant vimentin spin-labeled at these sites. No differences were seen between the EPR spectra from wild type and mutant vimentin for spin labels placed at residue 191. This suggested that the mutation did not alter the correct positioning of adjacent dimers centered at this residue in rod domain 1.

In contrast, comparison of wild type and mutant proteins labeled at residue 348, an indicator of anti-parallel overlap centered around this site in rod 2, revealed marked differences between wild type and R113S mutants. EPR spectra of the mutant showed no indication that proper alignment of these regions had occurred. Whether this failure to align was drastic or simply sufficient to displace the residue beyond the 2-nm limits of sensitivity for EPR is not yet known. In previous work we showed that the association between IF dimers at residue 191 (rod domain 1) occurs prior to that which occurs at 348 (rod domain 2), at least during *in vitro* assembly. Thus the data reported here would suggest that the initial lateral association between dimers centered around rod 1 is not detectably disturbed but that the association centered around rod 2 is. It is important to note, however, that these data are snapshots of small regions and cannot be used to make predictions on the

behavior of large segments of the molecule.

Also worth noting was the analysis of wild type and mutant proteins labeled at residue 131, a *d* position, in rod 1 closer to the site of the mutation. In both the wild type and R113S mutant, the 2 M urea spectra of spin-labeled residue 131 do not display the characteristic broad line shape of a *a/d* positions elsewhere in the molecule. The spectra are consistent with the assumption of α helical secondary structure at this site but not with the formation of coiled coil dimer. This observation is in agreement with the observations of Strelkov *et al.* (37), who examined crystals of vimentin sequence 102–138 of rod domain 1. Their analysis of rod 1A showed the presence of α helices but not coiled coils (37). These investigators postulated that this region might well form coiled coil in the native protein and that the absence of coiled coil in the crystals may have resulted from the fact that these fragments were removed from the context of the whole protein/filament. The data presented here would support an absence of coiled coil at this site, although spectra from additional sites need to be studied to establish a higher level of confidence. It is also worth noting that algorithms designed to predict secondary structure also show a greater degree of variability in the confidence with which coiled coil structure is predicted for this region of residues 106–139, predictions that are also consistent with no or minimized coiled coil structure (43, 44).

EPR spectra of spin-labeled IF proteins provide data that reveal structure at very specific sites within intact intermediate filaments. While such views lack the context and resolution that would be provided by crystal structure of intact filaments, they do offer data that directly addresses local structure in intact filaments under physiologic conditions. The data reported here suggest that the human vimentin R113S mutation, within the limits of resolution offered by SDSL EPR, does not affect either coiled coil formation, or the initial dimerization centered around rod 1, but does demonstrably alter the dimerization centered around rod 2. These data thus provide groundwork for continued studies on the normal and pathological structure of IFs.

REFERENCES

1. Bonifas, J. M., Rothman, A. L., and Epstein, E. H., Jr. (1991) *Science* **254,** 1202–1205
2. Brenner, M., Johnson, A. B., Boespflug-Tanguy, O., Rodriguez, D., Goldman, J. E., and Messing, A. (2001) *Nat. Genet.* **27,** 117–120
3. Chan, Y. M., Yu, Q. C., Fine, J. D., and Fuchs, E. (1993) *Proc. Natl. Acad. Sci. U. S. A.* **90,** 7414–7418
4. Chen, H., Bonifas, J. M., Matsumura, K., Ikeda, S., Leyden, W. A., and Epstein, E. H., Jr. (1995) *J. Invest. Dermatol.* **105,** 629–632
5. Cheng, J., Syder, A. J., Yu, Q. C., Letai, A., Paller, A. S., and Fuchs, E. (1992) *Cell* **70,** 811–819
6. Coleman, C. M., Hannush, S., Covello, S. P., Smith, F. J., Uitto, J., and McLean, W. H. (1999) *Am. J. Ophthalmol.* **128,** 687–691
7. Corden, L. D., Swensson, O., Swensson, B., Rochels, R., Wannke, B., Thiel, H. J., and McLean, W. H. (2000) *Br. J. Ophthalmol.* **84,** 527–530
8. Coulombe, P. A., and Fuchs, E. (1993) *Semin. Dermatol.* **12,** 173–190
9. Fuchs, E. (1991) *Biochem. Soc. Trans.* **19,** 1112–1115
10. Fuchs, E., and Coulombe, P. A. (1992) *Cell* **69,** 899–902
11. Fuchs, E. (1994) *J. Cell Biol.* **125,** 511–516
12. Syder, A. J., Yu, Q. C., Paller, A. S., Giudice, G., Pearson, R., and Fuchs, E. (1994) *J. Clin. Invest.* **93,** 1533–1542
13. Lane, E. B., Rugg, E. L., Navsaria, H., Leigh, I. M., Heagerty, A. H., Ishida-Yamamoto, A., and Eady, R. A. (1992) *Nature* **356,** 244–246
14. Shemanko, C. S., Mellerio, J. E., Tidman, M. J., Lane, E. B., and Eady, R. A. (1998) *J. Invest. Dermatol.* **111,** 893–895
15. Corden, L. D., Mellerio, J. E., Gratian, M. J., Eady, R. A., Harper, J. I., Lacour, M., Magee, G., Lane, E. B., McGrath, J. A., and McLean, W. H. (1998) *Hum. Mutat.* **11,** 279–285
16. Leigh, I. M., and Lane, E. B. (1993) *Arch. Dermatol.* **129,** 1571–1577
17. Rugg, E. L., Morley, S. M., Smith, F. J., Boxer, M., Tidman, M. J., Navsaria, H., Leigh, I. M., and Lane, E. B. (1993) *Nat. Genet.* **5,** 294–300
18. Chan, Y., Anton-Lamprecht, I., Yu, Q. C., Jackel, A., Zabel, B., Ernst, J. P., and Fuchs, E. (1994) *Genes Dev.* **8,** 2574–2587
19. Letai, A., Coulombe, P. A., McCormick, M. B., Yu, Q. C., Hutton, E., and Fuchs, E. (1993) *Proc. Natl. Acad. Sci. U. S. A.* **90,** 3197–3201
20. Vassar, R., Coulombe, P. A., Degenstein, L., Albers, K., and Fuchs, E. (1991) *Cell* **64,** 365–380
21. Coulombe, P. A., Hutton, M. E., Letai, A., Hebert, A., Paller, A. S., and Fuchs, E. (1991) *Cell* **66,** 1301–1311
22. Nishida, K., Honma, Y., Dota, A., Kawasaki, S., Adachi, W., Nakamura, T., Quantock, A. J., Hosotani, H., Yamamoto, S., Okada, M., Shimomura, Y., and Kinoshita, S. (1997) *Am. J. Hum. Genet.* **61,** 1268–1275
23. Irvine, A. D., Corden, L. D., Swensson, O., Swensson, B., Moore, J. E., Frazer, D. G., Smith, F. J., Knowlton, R. G., Christophers, E., Rochels, R., Uitto, J., and McLean, W. H. (1997) *Nat. Genet.* **16,** 184–187
24. Gupta, S. K., and Hodge, W. G. (1999) *Curr. Opin. Ophthalmol.* **10,** 234–241
25. Rodriguez, D., Gauthier, F., Bertini, E., Bugiani, M., Brenner, M., N'Guyen, S., Goizet, C., Gelot, A., Surtees, R., Pedespan, J. M., Hernandorena, X., Troncoso, M., Uziel, G., Messing, A., Ponsot, G., Pham-Dinh, D., Dautigny, A., and Boespflug-Tanguy, O. (2001) *Am. J. Hum. Genet.* **69,** 1134–1140
26. Cooper, D. N., and Youssoufian, H. (1988) *Hum. Genet.* **78,** 151–155
27. Mehrani, T., Wu, K. C., Morasso, M. I., Bryan, J. T., Marekov, L. N., Parry, D. A., and Steinert, P. M. (2001) *J. Biol. Chem.* **276,** 2088–2097
28. Wu, K. C., Bryan, J. T., Morasso, M. I., Jang, S. I., Lee, J. H., Yang, J. M., Marekov, L. N., Parry, D. A., and Steinert, P. M. (2000) *Mol. Biol. Cell* **11,** 3539–3558
29. Wawersik, M., Paladini, R. D., Noensie, E., and Coulombe, P. A. (1997) *J. Biol. Chem.* **272,** 32557–32565
30. Hess, J. F., Budamagunta, M. S., Voss, J. C., and FitzGerald, P. G. (2004) *J. Biol. Chem.* **279,** 44841–44846
31. Hess, J. F., Voss, J. C., and FitzGerald, P. G. (2002) *J. Biol. Chem.* **277,** 35516–35522
32. Carter, J. M., Hutcheson, A. M., and Quinlan, R. A. (1995) *Exp. Eye Res.* **60,** 181–192
33. Ma, L., Yamada, S., Wirtz, D., and Coulombe, P. A. (2001) *Nat. Cell Biol.* **3,** 503–506
34. Hess, J. F., Casselman, J. T., and FitzGerald, P. G. (1993) *Curr. Eye Res.* **12,** 77–88
35. Hess, J. F., Casselman, J. T., and FitzGerald, P. G. (1996) *J. Biol. Chem.* **271,** 6729–6735
36. Strelkov, S. V., Herrmann, H., Geisler, N., Lustig, A., Ivaninskii, S., Zimbelmann, R., Burkhard, P., and Aebi, U. (2001) *J. Mol. Biol.* **306,** 773–781
37. Strelkov, S. V., Herrmann, H., Geisler, N., Wedig, T., Zimbelmann, R., Aebi, U., and Burkhard, P. (2002) *EMBO J.* **21,** 1255–1266
38. McLean, W. H., Pulkkinen, L., Smith, F. J., Rugg, E. L., Lane, E. B., Bullrich, F., Burgeson, R. E., Amano, S., Hudson, D. L., Owaribe, K., McGrath, J. A., McMillan, J. R., Eady, R. A., Leigh, I. M., Christiano, A. M., and Uitto, J. (1996) *Genes Dev.* **10,** 1724–1735
39. Banwell, B. L., Russel, J., Fukudome, T., Shen, X. M., Stilling, G., and Engel, A. G. (1999) *Journal of Neuropathology and Exp. Neurol.* **58,** 832–846
40. Andra, K., Lassmann, H., Bittner, R., Shorny, S., Fassler, R., Propst, F., and Wiche, G. (1997) *Genes Dev.* **11,** 3143–3156
41. Herrmann, H., Wedig, T., Porter, R. M., Lane, E. B., and Aebi, U. (2002) *J. Struct. Biol.* **137,** 82–96
42. Smith, T. A., Steinert, P. M., and Parry, D. A. (2004) *Proteins* **55,** 1043–1052
43. Berger, B., Wilson, D. B., Wolf, E., Tonchev, T., Milla, M., and Kim, P. S. (1995) *Proc. Natl. Acad. Sci. U. S. A.* **92,** 8259–8263
44. Lupas, A., Van Dyke, M., and Stock, J. (1991) *Science* **252,** 1162–1164